



OPEN ACCESS

EDITED BY

Feng-Yan Bai,
Chinese Academy of Sciences (CAS), China

REVIEWED BY

Heng-Lin Cui,
Jiangsu University, China
Min Yu,
Ocean University of China, China

*CORRESPONDENCE

Cong Sun
✉ michaelLsc@sina.com

RECEIVED 27 June 2023

ACCEPTED 26 September 2023

PUBLISHED 20 October 2023

CITATION

Gao J-W, Ying J-J, Dong H, Liu W-J,
He D-Y, Xu L and Sun C (2023)
Characterization of *Maribacter*
polysaccharolyticus sp. nov., *Maribacter*
huludaoensis sp. nov., and *Maribacter*
zhoushanensis sp. nov. and illumination
of the distinct adaptative strategies of
the genus *Maribacter*.
Front. Mar. Sci. 10:1248754.
doi: 10.3389/fmars.2023.1248754

COPYRIGHT

© 2023 Gao, Ying, Dong, Liu, He, Xu and
Sun. This is an open-access article
distributed under the terms of the [Creative
Commons Attribution License \(CC BY\)](https://creativecommons.org/licenses/by/4.0/). The
use, distribution or reproduction in other
forums is permitted, provided the original
author(s) and the copyright owner(s) are
credited and that the original publication in
this journal is cited, in accordance with
accepted academic practice. No use,
distribution or reproduction is permitted
which does not comply with these terms.

Characterization of *Maribacter polysaccharolyticus* sp. nov., *Maribacter huludaoensis* sp. nov., and *Maribacter zhoushanensis* sp. nov. and illumination of the distinct adaptative strategies of the genus *Maribacter*

Jia-Wei Gao^{1,2}, Jun-Jie Ying^{1,2}, Han Dong¹, Wen-Jia Liu^{1,2},
Dong-Yan He¹, Lin Xu^{1,2} and Cong Sun^{1,2*}

¹College of Life Sciences and Medicine, Zhejiang Sci-Tech University, Hangzhou, China, ²Shaoxing Biomedical Research Institute of Zhejiang Sci-Tech University Co., Ltd, Zhejiang Engineering Research Center for the Development Technology of Medicinal and Edible Homologous Health Food, Shaoxing, China

Polysaccharides are complex carbohydrates and are abundant in the marine environment. Microbes degrade and utilize them using Carbohydrate-active enzymes (CAZymes), which mediate polysaccharides into the marine carbon cycle. With the continued supply of polysaccharides from the marine environment, tidal flats are also abundant in polysaccharides, resulting in an abundance of marine polysaccharide degrading strains. In this study, three novel strains, designated as D37^T, M208^T, and SA7^T, were isolated from the intertidal sediment samples located in Zhoushan, Zhejiang and Huludao, Liaoning, PR China. The phylogenetic trees using the 16S rRNA gene and genome sequences showed that the three novel strains belonged to the genus *Maribacter*. The highest 16S rRNA gene sequence similarities between the three novel strains and other strains of the genus *Maribacter* were 98.7%, 99.2%, and 98.8%, respectively, while the ANI, AAI, and dDDH values between the three strains and the other strains of the genus *Maribacter* were 70-86%, 67-91%, and 17-30%, respectively, supporting their affiliation as novel species. Combined with other phenotypic and genotypic characterization in this study, three novel species are proposed as *Maribacter polysaccharolyticus* sp. nov., *Maribacter huludaoensis* sp. nov., and *Maribacter zhoushanensis* sp. nov., respectively, for the three strains. Furthermore, we compared all available genomes of *Maribacter* representatives and found that *Maribacter* strains could be divided into two groups (A and B). The two groups are different in genome size and G + C content and gene densities of CAZyme, peptidase, and sulfatase. Group A possesses

more CAZymes which are related to degrading laminarin, fucoidan, mannan, xylose, and xylan. This result suggests that the two groups may have different niche adaptation strategies. Our study contributes to a better understanding of the role of marine flavobacteria in biogeochemical cycles and niche specialization.

KEYWORDS

tidal flats, bacteroidota, *Maribacter*, CAZyme, PUL, ecological niches

1 Introduction

Tidal flats, the boundary between the terrestrial and marine habitats, are well-known ecosystems for their productivity and possession of one of the most abundant and diverse microbial community (Schuerch et al., 2019; Niu et al., 2022). *Bacteroidota* is considered as a major part of bacterial communities in the tidal flats and plays an important role, participating in complex polysaccharides degradation, cycling of nutrients, carbon sequestration, and other functions (Zhang et al., 2018b). *Flavobacteriaceae*, one of the most important and largest components of this phylum, contains more than 160 validly published genera (Gavriilidou et al., 2020). *Maribacter*, of family *Flavobacteriaceae*, was initially identified and established with *Maribacter sedimenticola* (Nedashkovskaya et al., 2004). Based on the LPSN (<https://lpsn.dsmz.de/genus/maribacter>), there are 32 validly published species in the genus *Maribacter*. *Maribacter* species have been isolated from different marine environments such as tidal flats (Lo et al., 2013; Jung et al., 2014; Park et al., 2016; Thongphrom et al., 2016; Liu et al., 2020), seawater (Yoon et al., 2005; Barbeyron et al., 2008; Nedashkovskaya et al., 2010; Jin et al., 2017; Kang et al., 2018), marine sponges (Jackson et al., 2015), deep-sea sediment (Fang et al., 2017), and marine alga (Nedashkovskaya et al., 2007; Zhang et al., 2009; Weerawongwiwat et al., 2013; Khan et al., 2020; Zhang et al., 2020). *Maribacter* strains share similar characteristics such as containing menaquinone-6 (MK-6) as the major isoprenoid quinone (Zhang et al., 2020).

Algal polysaccharide is one of the most important components of marine organic carbon (Barbeyron et al., 2016). *Bacteroidota* usually utilizes algal polysaccharides through polysaccharide utilization loci (PUL), which are mainly comprised of carbohydrate-active enzymes (CAZymes), TonB-dependent receptor-like transporter (susC), and polysaccharide binding protein (susD) (Bennke et al., 2016). Besides, CAZymes encompass glycoside hydrolases (GH), polysaccharide lyases (PL), carbohydrate esterases (CE), auxiliary activity (AA), carbohydrate-binding modules (CBM), and glycosyl transferases (GT). The frequent transfer of CAZyme-encoding genes among microorganisms is an effective mechanism for strains to adapt to different environments and related niches (Arnosti et al., 2021). Recent studies suggest that *Flavobacteriaceae* is a major contributor to marine polysaccharide degradation and related carbon cycling in

the marine environment (Klippel et al., 2011; Mann et al., 2013; Sun et al., 2020). For example, *Zobellia galactanivorans* is able to degrade diverse marine polysaccharides including alginate, carrageenan, and laminarin and is capable of complex degradation and regulatory mechanisms for the species that have been revealed (Ficko-Blean et al., 2017; Zhu et al., 2017). *Formosa agariphila* can degrade ulvan through related PUL (Reisky et al., 2019). *Maribacter* is one of the recurrent genera in a highly dynamic fashion of a bacterial community in the North Sea spring blooms (Bartlau et al., 2022). The analysis of CAZyme and PUL in a novel strain *Maribacter dokdonensis* 62-1 indicated that it was specialized to certain “polysaccharide niches” such as alginate and ulvan (Wolter et al., 2021).

In this study, three novel isolates D37^T, M208^T, and SA7^T were discovered in the intertidal sediments of Zhoushan and Huludao, China, and subject to polyphasic taxonomic identification. We also compared the genomes of the three novel isolates with all available strains of the genus *Maribacter* to clarify their similarities and differences in algal polysaccharide degradation, and tried to illuminate their preference in carbon cycles and niche specialization. Through this study, we provide novel resources of the genus *Maribacter* and further evidence for its evolution. The result is valuable for our understanding of the role of marine flavobacteria in biogeochemical cycles and niche specialization.

2 Materials and methods

2.1 Strain isolation and cultivation

A self-manufactured columnar tube sampler was used to collect and stratify the sediment samples, collected samples at varying depths (0-5, 5-15, and 15-30 cm) were immediately kept at 4°C in sterile self-sealing bags before reservation (Wu et al., 2021). The sediment samples were preserved at 4°C for short-term preservation and preserved at -20°C for long-term preservation. The sediment sample was 10-fold serially diluted to 10⁻³ with 3% NaCl solution, and 50 µl diluent was coated on the marine agar 2216 with 1/10 strength of yeast extract and peptone (MA; Becton Dickinson) to minimize the isolation of fast-growing strains, which usually belong to well-studied species, and maximize the isolation of rarely studied strains in the samples. The strains were picked out after five days of

incubation at 25°C and purified by subcultivation on marine agar 2216 at 25°C. The novel strains were frozen at -80°C, supplemented with glycerol (25%, v/v) for long-term preservation, and cultivated in marine broth (MB, Becton Dickinson) for three days for further experiments. Strains D37^T and SA7^T were isolated from intertidal sediments collected in Zhoushan, Zhejiang, PR China (21°35' N, 109°80' E) and strain M208^T was isolated from an intertidal sediment sample collected in Huludao, Liaoning, PR China (40° 41' N, 120°56' E).

2.2 Morphological, physiological, biochemical, and chemotaxonomic features

The colony morphology was viewed by scribing on MA after 3 days. Transmission electron microscopy (TEM, JEM-1400Flash) was used to examine the cell morphology of novel isolates incubated at MA after 3 days. The Gram staining method was used to detect the Gram reaction. (Romero et al., 1988). Motility was observed by dipping a small amount of bacterial solution into a semi-solid culture medium (MA, reduce 0.5% agar content) with an inoculation needle and cultivating the bacterial solution under optimal conditions for 3 days. Anaerobic growth was tested using the formulated anaerobic culture medium as described (Xu et al., 2021). The activities of catalase and oxidase were tested as described (Sun et al., 2018). To determine the growth ranges and optimal conditions, the temperature ranges (4, 10, 15, 20, 25, 27, 30, 37, 40, 42, 45, 50 °C), pH range (5.0 to 10.0), and different NaCl concentrations (0, 0.5, 1.0, 1.5, 2.0, 2.5, 3.0, 3.5, 4.0, 6.0, 8.0, 10.0, and 12.0%, w/v) for growth were investigated as described (Gao et al., 2023). Hydrolysis of starch, tyrosine, cellulose, Tween 20, 40, 60, and 80, and casein were tested in modified MA (MA medium without peptidase and with reduced yeast extract of 0.1 g/L) and then with added 2g/L starch, 5g/L tyrosine, 10g/L Tween 20, 40, 60, and 80 each, 2g/L cellulose and 10g/L casein, respectively (Sun et al., 2018). API 20NE, API ZYM, and API 50CH strips (bioMérieux) were utilized for physiological, biochemical and acid production, respectively, according to the instruction manuals.

The cells of strains D37^T, M208^T, and SA7^T for the analysis of fatty acids were collected after being cultivated on MA at optimum temperature for 3 days, then subjected to gas chromatography (Agilent 8860). The results were analyzed with the Sherlock microbial identification system (MIDI) and the standard MIS library generation software (version 6.5) (Gao et al., 2023). Polar lipids were extracted following the described procedure (Ying et al., 2021), separated on the TLC silica gel plate (60 F254, Merck, 10 x 10 cm, activate in 55 °C oven for 30 minutes) by two-dimensional TLC, and finally visualized by spraying staining agents including phosphomolybdic acid for total lipids, ninhydrin for amino lipids, molybdenum blue for phospholipids, alpha-naphthol with sulfuric acid for glycolipids to distinguish different polar lipids (Sun et al., 2019; Ying et al., 2021). The respiratory quinones were analyzed using one-dimensional TLC and High Performance Liquid Chromatography

(HPLC; Agilent 1200) and Mass Spectrometry (MS; Thermo Finnigan LCQ DECA XP MAX) as described (Sun et al., 2014).

2.3 Genome sequencing and phylogenetic analyses

Genomic DNA was extracted as described (Sun et al., 2016) and sent to Guangdong Magigene Biotechnology Co. Ltd. (Guangzhou, PR China) for genome sequencing. Illumina Hiseq platform (Novaseq 6000) and SPAdes v.3.10.1 were used for the genome sequencing and assembly, respectively. CheckM v.1.0.7 was used to estimate the quality of the spliced genome (Parks et al., 2015). The complete 16S rRNA gene sequences were extracted from the genome data by the RNAmmer v.1.2 (Lagesen et al., 2007), and further confirmed using Sanger sequencing by Tsingke Biotechnology Co., Ltd. (Beijing, PR China). Sequence similarities were compared by using the EzBioCloud (www.ezbiocloud.net) and the 16S rRNA genes of closely related type strains were downloaded from NCBI and analyzed using the MEGA 11.0 software with ClustalW program (Tamura et al., 2021) for sequence alignment. The neighbor-joining (NJ) (Saitou and Nei, 1987), maximum-likelihood (ML) (Felsenstein, 1981), maximum-parsimony (MP) (Fitch, 1971), and minimum-evolution (ME) (Rzhetsky and Nei, 1992) methods were used for the reconstruction of phylogenetic trees. For all methods, the Kimura's two-parameter model (Kimura, 1980) and 1000 replications were employed (Do, 1992). *Zeaxanthinibacter aestuarii* S2-22^T was used as an outgroup.

For phylogenomic analysis, twenty-two genomes of type strains in the genus *Maribacter* were downloaded from NCBI (<https://www.ncbi.nlm.nih.gov>), *Zeaxanthinibacter enoshimensis* DSM 18435^T was used as an outgroup. Together with the draft genomes of strains D37^T, M208^T, and SA7^T, all genomes (Table S1) were annotated by the RAST server (Aziz et al., 2008). OrthoFinder v.2.5.4 was used for the extraction of orthologous clusters (OCs) of all genomes based on protein sequences, single-copy orthologous clusters were unified by MAFFT v.7.490 (Katoh and Standley, 2013), and then refined with trimAL v.1.2.rev59 (Capella-Gutierrez et al., 2009). The Local Perl script "concatenate.pl" was used for sequence concatenation. The '-m MFP' was served as a predictive command of the best amino acid substitution model of concatenated sequences in IQ-TREE v.1.6.12, for which, 'LG+F+I+R5' was used as the best amino acid model in this study. Based on the amino acid model 'LG+F+I+R5', the maximum-likelihood phylogenomic tree with ultrafast bootstraps set to 1,000 was reconstructed by IQ-TREE. tvBOT web application was applied for visualizing and modifying phylogenetic trees (Xie et al., 2023). The values of average nucleotide identity (ANI), the digital DNA-DNA hybridization (dDDH) and Average Amino acid Identity (AAI) were analyzed by OrthoANI Tool version 0.93.1 (Kim et al., 2014) (Lee et al., 2016), Genome-to-Genome Distance Calculator 3.0 web server (<https://ggdc.dsmz.de/ggdc.php#>) (Meier-Kolthoff et al., 2013), and the AAI Calculator (<http://enve-omics.ce.gatech.edu/aai/>) (Chun et al., 2018), respectively.

2.4 Comparative genomic analyses

The metabolic genes and pathways were annotated and analyzed in the KEGG website (<https://www.kegg.jp/blastkoala/>) (Kanehisa et al., 2017). Functional annotations assigned to Clusters of Orthologous groups (COG) were performed with the eggno-mapper version 2 (Cantalapiedra et al., 2021). CAZyme was identified using dbCAN2 (<https://bcb.unl.edu/dbCAN2/blast.php>) (Zhang et al., 2018a). Peptidase was annotated against MEROPS (<https://www.ebi.ac.uk/merops/>) (Rawlings et al., 2018) and the local server BLASTP (only considering values $e < 1e-15$). Sulfatase was identified using the database of Sulfatases SulfAtlas version 2.3.1 (<https://sulfatlas.sb-roscoff.fr/sulfatlas/>) (Stam et al., 2023) and the local server BLASTP (only considering values of $e < 1e-15$). PUL and its function genes were predicted based on the PULDB databases (<http://www.cazy.org/PULDB/>) (Terrapon et al., 2018). Data were visualized by chipLOT (<https://www.chipLOT.online>). The principal component analysis (PCA) was performed in RStudio using R v4.1.2 and visualized using the package prompts.

3 Results and discussion

3.1 Morphological, physiological, biochemical, and chemotaxonomic characteristics

Strains D37^T, M208^T, and SA7^T were all Gram-stain-negative, rod-shaped, aerobic, and non-motile, which were similar to other *Maribacter* strains. The cells of strains D37^T, M208^T, and SA7^T were rod-shaped with 1.8–3.3, 1.7–2.7, and 1.5–3 μm in length, and 0.4–0.8, 0.3–0.4, and 0.6–0.8 μm in width, respectively (Figure S1). The three strains all formed yellow, round, opaque, border smooth, and convex colonies after scribing on MA medium and cultivated for 3 days. Strain D37^T was observed to be oxidase-positive and catalase-positive as most *Maribacter* strains, but strain M208^T and SA7^T were both weakly positive in oxidase and negative in catalase. Strains D37^T, M208^T, and SA7^T could all hydrolyze tyrosine and Tween 20, and none of them could hydrolyze casein. Besides, the three strains showed different reactions in starch, cellulose, and Tween 40, 60, and 80 hydrolysis. Strains M208^T and SA7^T could hydrolyze cellulose, Tween 40, 60, and 80, but strain D37^T could not. On the contrary, only strain D37^T could hydrolyze starch. Moreover, the three strains also differed in other biochemical characteristics, including the fermentation of glucose, esterase (C4), esterase lipase (C8), cysteine arylamidase, trypsin, chymotrypsin, α -galactosidase, α -mannosidase, α -glucosidase, β -galactosidase, β -fucosidase, glycerol, D-arabinose, L-fucose, D-fructose, D-mannose, N-acetyl-glucosamine, D-mannitol, starch, and so on. In general, strain D37^T exhibited stronger enzyme activity and carbohydrate acid production ability. The detailed features differentiating strains D37^T, M208^T, and SA7^T from their closely related *Maribacter* strains are shown in Table 1.

The major fatty acids (>10%) of strains D37^T, M208^T, and SA7^T were iso-C_{15:0} (16.7%, 14.4%, 13.2%, respectively) and iso-C_{17:0} 3-OH (16.3%, 16.6%, 25.3%, respectively), which were all detected in

other members of the genus *Maribacter* as the major fatty acids (Table 2). Meanwhile, fatty acids C_{16:0}, iso-C_{13:0}, iso-C_{14:0}, anteiso-C_{15:0}, iso-C_{15:1} G, C_{16:0} 3-OH, iso-C_{15:0} 3-OH, iso-C_{16:0} 3-OH, Summed Feature 3, and Summed Feature 9 were determined for strains D37^T, M208^T, and SA7^T as the minor fatty acids (>1% but <10%, Summed Feature 3 in strain M208^T was >10%). Strain D37^T had more differences to strains M208^T and SA7^T including iso-C_{15:1} G, anteiso-C_{15:0}, and Summed Feature 1. The fatty acid iso-C_{15:1} G was only detected in strain D37^T, and the content of anteiso-C_{15:0} in strain D37^T was clearly more than the other two strains. The fatty acid profiles of strains M208^T and SA7^T were quite similar. Summed Feature 1 was only detected in strains M208^T and SA7^T, while these two strains also had minor differences such as C_{16:0} and C_{15:0} 3-OH. The detailed fatty acid results of strains D37^T, M208^T and SA7^T with their closely related taxa of the genus *Maribacter* are in Table 2. The major polar lipids of strains D37^T, M208^T, and SA7^T all comprised phosphatidylethanolamine (PE), unidentified glycolipids (GL), unidentified aminolipids (AL), and unidentified lipids (L), which resembled the majority of *Maribacter* strains (Table 1, Figure S2). Strain D37^T and its reference strain *M. luteus* RZ05^T both consisted of PE, two GLs, and one AL, and *M. luteus* RZ05^T had one additional unidentified lipid compared to strain D37^T. Like its reference strain *M. dokdonensis* DSW-8^T, strain M208^T also contained PE and one AL, but compared with each other, *M. dokdonensis* DSW-8^T had two additional unidentified phospholipids (PL) and strain M208^T had one GL. The polar lipid profile of strain SA7^T was also similar to its reference strain *M. caenipelagi* HD-44^T. However, strain *M. caenipelagi* HD-44^T was absent of GL and had an extra unidentified lipid. Similar to the majority of bacteria in the genus *Maribacter*, the major respiratory quinone of strains D37^T, M208^T, and SA7^T was MK-6.

According to the above phenotypical features, these three strains showed common features of the genus *Maribacter* but also features that are distinct from them. Three strains shared similar chemotaxonomic features such as MK-6 as the major respiratory quinone, iso-C_{15:0} and iso-C_{17:0} 3-OH as the major fatty acids, and PE as the main polar lipid with *Maribacter* strains, while the oxidase, catalase, hydrolysis of starch, cellulose, Tween 40, 60, and 80, and other physiological and biochemical characteristics indicated that these three strains as well as the genus *Maribacter* were clearly distinct. Therefore, these three strains could be classified as novel species of the genus *Maribacter* based on their phenotypical characteristics.

3.2 Phylogenetic analyses based on 16S rRNA gene and genome sequences

The lengths of the complete 16S rRNA gene of strains D37^T, M208^T, and SA7^T were 1535, 1537, and 1533 bp, respectively. Strain D37^T showed the highest 16S rRNA gene sequence identities with *M. luteus* RZ05^T (98.76%), followed by *M. polysiphoniae* LMG 23671^T (97.24%), *M. arenosus* CAU 1321^T (96.93%), *M. maritimus* HMF 3635^T (96.83%), and the rest of *Maribacter* type strains (<95.85%). The 16S rRNA gene sequence of strain M208^T was most closely similar with *M. dokdonensis* DSW-8^T (99.17%), then

TABLE 1 Characteristics that differentiate strains D37^T, M208^T, and SA7^T from closely related taxa of the genus.

Characteristic	1	2	3	4 ^a	5 ^b	6 ^c	7 ^d
Temperature range (°C) for growth	15-37	4-35	4-30	7-40	4-35	4-32	4-35
pH range for growth	5.5-8.5	6.0-8.5	5.5-9	5.5-9	5.5-8	5.5-8.5	5.5-8
NaCl concentration (%) for growth	0-6	0.5-6	0.5-6	0.5-6	0.5-10	0-9	0-10
Oxidase	+	w	w	+	+	-	+
Catalase	+	-	-	+	+	+	-
Hydrolysis of							
starch	+	-	-	+	-	-	-
cellulose	-	+	+	-	ND	ND	ND
Tween 40	-	+	+	+	+	+	+
Tween 60	-	+	+	+	+	ND	+
Tween 80	-	+	+	+	+	+	+
API 20NE:							
fermentation of glucose	+	-	-	+	ND	ND	ND
API ZYM:							
Esterase (C4) and Esterase lipase (C8)	w	w	+	+	+	+	+
cysteine arylamidase	w	w	-	+	-	+	-
trypsin	+	w	-	+	-	-	-
chymotrypsin	w	+	w	+	-	+	+
α-galactosidase	-	w	w	+	-	+	+
β-galactosidase and α-glucosidase	-	+	+	+	-	+	+
β-fucosidase	w	-	-	ND	ND	ND	ND
API 50CH							
Glycerol, D-arabinose and L-fucose	+	-	-	ND	ND	ND	ND
D-fructose, D-mannose and N-acetyl-glucosamine	+	w	+	ND	ND	ND	ND
D-mannitol, starch and potassium 2-ketogluconate	+	-	+	ND	ND	ND	ND
methyl- αD-mannopyranoside, inulin and D-melezitose	+	w	w	ND	ND	ND	ND
glycogen and xylitol	+	-	w	ND	ND	ND	ND
potassium gluconate	-	+	+	ND	ND	ND	ND
L-rhamnose	-	+	-	ND	ND	ND	ND
Methyl-βD-xylopyranoside	-	w	w	ND	ND	ND	ND
Polar lipids	PE, GL (2), AL, L (3)	PE, GL (2), AL, L (2)	PE, GL (3), AL, L (2)	PE, GL (2), AL, L (4)	PE, GL (1), PL (2), AL	ND	PE, AL, L (5)
DNA G+C% content (%)	41.7	35.9	34.8	38.9	36.1	34.4	37.6

Strains: 1, strain D37^T; 2, strain M208^T; 3, strain SA7^T; 4, *M. luteus* RZ05^T; 5, *M. dokdonensis* DSW-8^T; 6, *M. forsetii* KT02ds18-4^T.

+, Positive; -, Negative; w, weakly positive; ND, not detected; PE, phosphatidylethanolamine; GL, glycolipids; AL, aminolipid; PL, phospholipid; L, Lipid. Data were cited from ^aLiu et al. (2020), ^bYoon et al. (2005), ^cBarbeyron et al. (2008), ^dJung et al. (2014).

M. confluentis SSK2-2^T (97.73%), *M. litoralis* SDRB-Phe2^T (97.69%), *M. stanieri* KMM 6046^T (97.58%), and less than 97.51% with other type species. Strain SA7^T was identified to have the highest identities of 98.69% 16S rRNA gene sequence with *M.*

forsetii KT02ds18-6^T, followed by *M. litoralis* SDRB-Phe2^T (98.67%), *M. spongiicola* W15M10^T (98.35%), *M. ulvicola* KMM 3951^T (98.34%), and the rest of the strains of *Maribacter* (<98.13%). From the above results, the similarity of 16S rRNA gene sequence

TABLE 2 Comparison of cellular fatty acid compositions of novel isolates and closely related taxa of the genus *Maribacter*.

Fatty acids	1	2	3	4 ^a	5 ^b	6 ^c
Straight-chain						
C _{14:0}	TR	1.5	TR	-	2.0	TR
C _{16:0}	5.3	6.0	1.8	TR	5.2	3.4
Unsaturated						
C _{15:1} ω6c	TR	TR	1.7	3.1	-	1.6
C _{17:1} ω6c	TR	TR	1.1	TR	-	TR
Branched-chain						
iso-C _{13:0}	1.6	1.5	1.4	-	TR	1.2
iso-C _{14:0}	3.4	5.7	5.3	-	-	4.8
iso-C _{15:0}	16.7	14.4	13.2	19.6	26.7	10.3
iso-C _{15:1} G	9.0	-	-	18.9	16.0	-
iso-C _{16:0}	1.2	1.2	TR	-	-	1.1
anteiso-C _{14:0}	1.1	TR	TR	-	-	2.2
anteiso-C _{15:0}	6.8	1.9	1.0	5.2	1.3	-
Hydroxy						
C _{15:0} 3-OH	-	TR	1.9	1.7	1.4	1.6
C _{16:0} 3-OH	1.5	5.7	2.7	TR	5.4	4.3
C _{17:0} 2-OH	2.7	TR	TR	1.7	-	-
iso-C _{14:0} 3-OH	TR	TR	-	-	-	-
iso-C _{15:0} 3-OH	5.4	5.3	5.8	7.5	4.2	4.3
iso-C _{16:0} 3-OH	5.0	3.2	3.6	7.8	1.0	4.4
iso-C _{17:0} 3-OH	16.3	16.6	25.3	10.5	26.4	20.4
Summed Feature 1	-	14.4	14.2	-	-	13.5
Summed Feature 3	8.9	10.2	7.9	6.4	9.5	13.0
Summed Feature 9	5.2	1.9	4.3	7.9	2.2	4.8

Data of strains were taken from ^aLiu et al. (2020), ^bJung et al. (2014), ^cZhang et al. (2020).

Summed feature 1 contains iso-C_{15:1} H and/or C_{13:0} 3-OH; Summed feature 3 contains C_{16:1} ω7c and/or C_{16:1} ω6c; Summed feature 9 contains 10-methyl C_{16:0} and/or iso-C_{17:1} ω9c. Strains: 1, strain D37^T; 2, strain M208^T; 3, strain SA7^T; 4, *M. luteus* RZ05^T; 5, *M. dokdonensis* DSW-8^T; 6, *M. spongiicola* DSM 25233^T.

Values are percentages of total fatty acids. Fatty acids representing >10% of the total are in bold type. -, not detected. TR, traces (<0.5%).

between the three strains and the type species of the genus *Maribacter* were higher than the recommended species delineation (98.65%), so we compared their ANI, AAI, and dDDH values with the other strains of the genus *Maribacter* (Figure 1). The ANI values between strains D37^T, M208^T, SA7^T and the species of the genus *Maribacter* ranged from 70% to 80%, 70% to 85%, and 70% to 86%, respectively. The AAI values and dDDH values of the three novel strains with other members of the genus *Maribacter* ranged from 17% to 23% and 66% to 83%, 17% to 29% and 67% to 90%, as well as 17% to 30% and 67% to 91%, respectively. According to the threshold values of recommended species delineation (ANI of < 95%; AAI of < 95%; dDDH of < 70%), the above results undoubtedly indicate that the three strains represent the new members of the genus *Maribacter* and are different species.

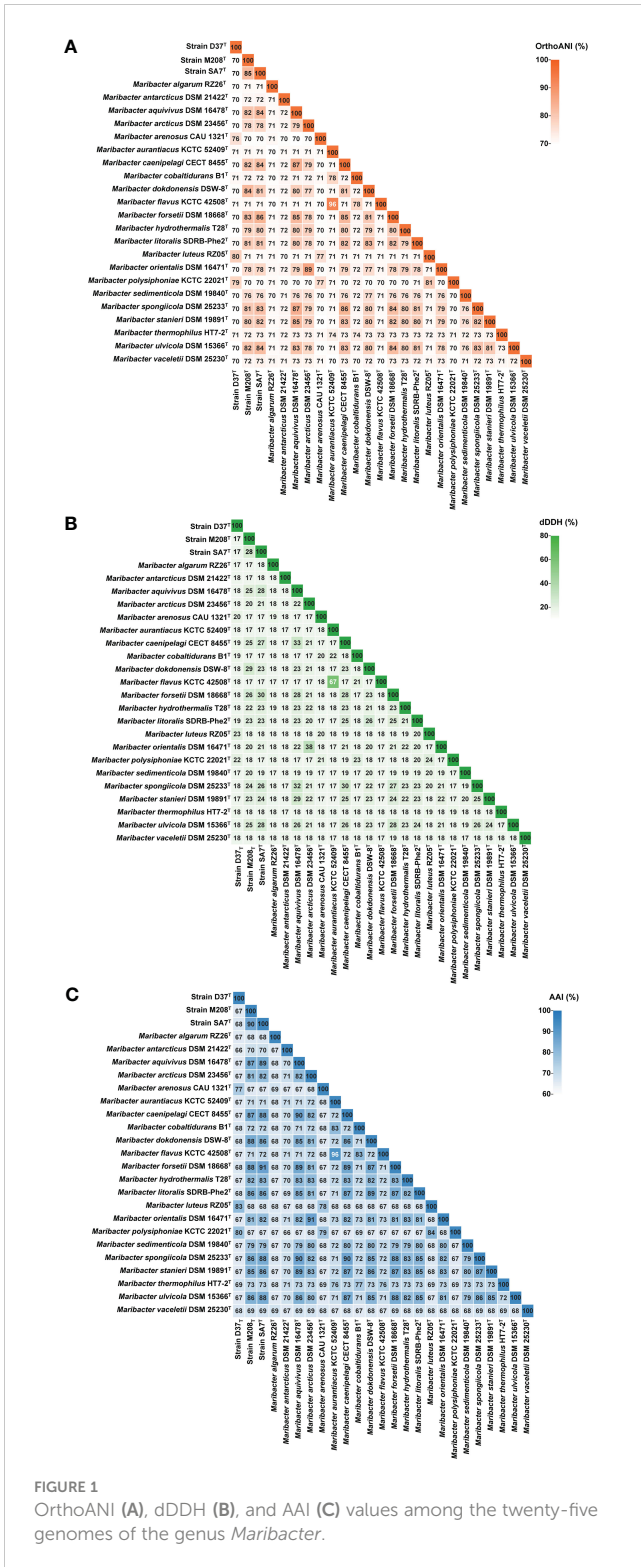
The phylogenetic trees reconstructed based on 16S rRNA gene sequences showed that strains D37^T, M208^T, and SA7^T were clustered with the members of the genus *Maribacter*, which firmly suggested that these three strains should be the new species of the genus *Maribacter* (Figure 2; Figures S3–S5). In the phylogenomic tree based on the single-copy orthologous proteins, the three strains were still situated in the genus *Maribacter*, supporting the affiliation of the three strains as the novel species of the genus *Maribacter* (Figure S6). Besides, these three strains were far apart from each other in the 16S rRNA phylogenetic trees, but in the phylogenomic tree, strains M208^T and SA7^T had a closer genetic relationship and were clustered in a clade far away from strain D37^T.

Although the highest similarity of 16S rRNA was higher than 98.65%, the value of recommended species delineation, their ANI,

3.3 General genomic features

The draft genome sequences of strains D37^T (GCF_014610845.1), M208^T (GCF_029350945.1), and SA7^T (GCF_029350975.1) had 21 contigs with 4,760,098 bp length and the *N*₅₀ value was 577,838 bp, 16 contigs with a length of 4,243,569 bp and the *N*₅₀ value was 341,292 bp, and 18 contigs with a length of 4,257,159 bp and the *N*₅₀ value was 844,229 bp, respectively. The genomic completeness and contamination values of strains D37^T, M208^T, and SA7^T were estimated to be 99.67% and 1.67%, 99.67% and 1.67%, and 99.67% and 0.33%, respectively. The genome size of strain D37^T was larger than strains M208^T and SA7^T, which were 4.8 Mb, 4.2 Mb, and 4.2 Mb, respectively, which were similar to the genome size of *Maribacter* species (ranges from 3.9 Mb to 5.1 Mb). The DNA G + C contents of strains D37^T, M208^T, and SA7^T calculated from the genome sequences were 41.7%, 35.9%, and 34.8%, respectively. Although the DNA G + C content of strain D37^T was higher than that of strains M208^T and SA7^T, it was still within the range for the genus *Maribacter* (31.7% ~ 41.8%). The detailed results of the genus *Maribacter* are shown in [Supplementary Table S1](#).

Metabolic pathway analysis based on the KEGG database indicated that these three strains all had metabolism pathways that could maintain the most basic life activities of organisms like the other *Maribacter* strains, including glycolysis, trichloroacetic acid (TCA) cycle, and fatty acid biosynthesis ([Figure S7](#)). Besides, strain D37^T had additional different metabolic pathways including nicotinamide adenine dinucleotide (NAD) biosynthesis, pyruvate metabolism, and cysteine biosynthesis. For example, only strain D37^T contained *nadA* and *nadB* genes that could biosynthesize the NAD from aspartate as well as *ppdk* genes that enabled the transformation of malate to phosphoenolpyruvate (PEP) ([Figure S8](#)). Strain SA7^T had a unique metabolic pathway that could degrade D-galacturonate, which was different from strain M208^T. The detailed results of clusters of orthologous groups (COG) are shown in [Figure 3](#). The top five gene functions with the highest proportion of the three strains were cell wall/membrane/envelope biogenesis (M), carbohydrate transport and metabolism (G), inorganic ion transport and metabolism (P), amino acid transport and metabolism (E), and energy production and conversion (C). However, strain D37^T contained more genes in energy production and conversion (C), carbohydrate transport and metabolism (G), inorganic ion transport and metabolism (P), and defense mechanisms (V). The number counts of CAZyme, sulfatase, and peptidase in strain D37^T were higher than those in strains M208^T and SA7^T (226 vs 156 vs 115, 377 vs 267 vs 212, 286 vs 235 vs 245, respectively). In addition, the quantities of CAZyme and sulfatase of strain D37^T were the highest and the second highest among the genus *Maribacter*, respectively and strain SA7^T had the lowest number counts of CAZyme and sulfatase ([Supplementary Table S2](#)). The number counts of peptidase of the genus *Maribacter* ranged from 189 to 380 and the three strains were all within the range.



AAI, and dDDH were below the threshold. Together with the 16S rRNA gene and genomic phylogenetic analysis above, strains D37^T, M208^T, and SA7^T could be assigned as the novel species of the genus *Maribacter*.

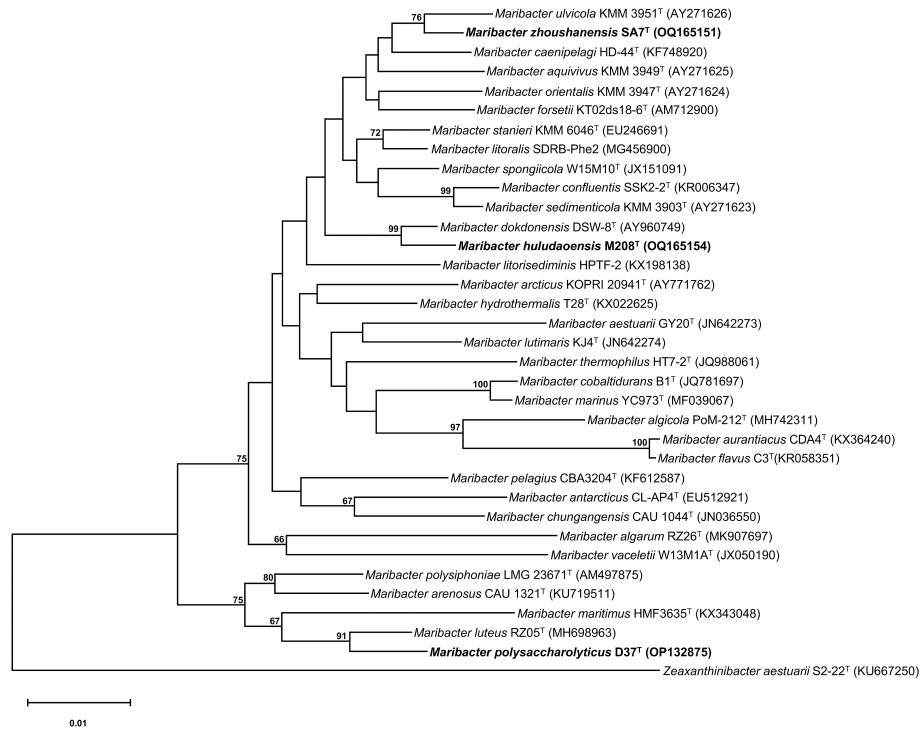


FIGURE 2
Neighbor-joining phylogenetic tree reconstructed with 16S rRNA gene sequences showing the relationships between strains D37^T, M208^T, and SA7^T and related taxa. Filled circles indicate branches recovered with both two methods (neighbor-joining and maximum-likelihood). Bootstrap values are based on 1000 replicates and values less than 65% are not shown. Bar, 0.01 substitutions per amino acid position. *Zeaxanthinibacter aestuarii* S2-22^T (KU667250) was used as an outgroup.

3.4 Comparative genomic analyses

3.4.1 *Maribacter* strains could be separated into two groups based on the genomic features

We performed a comparative genomic analysis of the genus *Maribacter*, including annotating the CAZyme, peptidase, and sulfatase in this genus and calculated their gene densities, which were the ratios of CAZyme, peptidase, and sulfatase to genome size,

respectively. (Supplementary Table S2). The CAZyme gene densities of the twenty-five *Maribacter* members ranged from 28 to 56 per/Mb. Among them, four strains including *M. arenosus* CAU121^T, *M. polysiphoniae* KCTC 22021^T, strain D37^T, and *M. luteus* RZ05^T, showed higher CAZyme gene densities which were 45, 44, 47, and 56 per/Mb, respectively. The CAZyme gene densities of the other eighteen strains ranged from 28 to 39 per/Mb except *M. algarum* RZ26^T, *M. vaceletti* DSM 25230^T, and *M. antarcticus* DSM

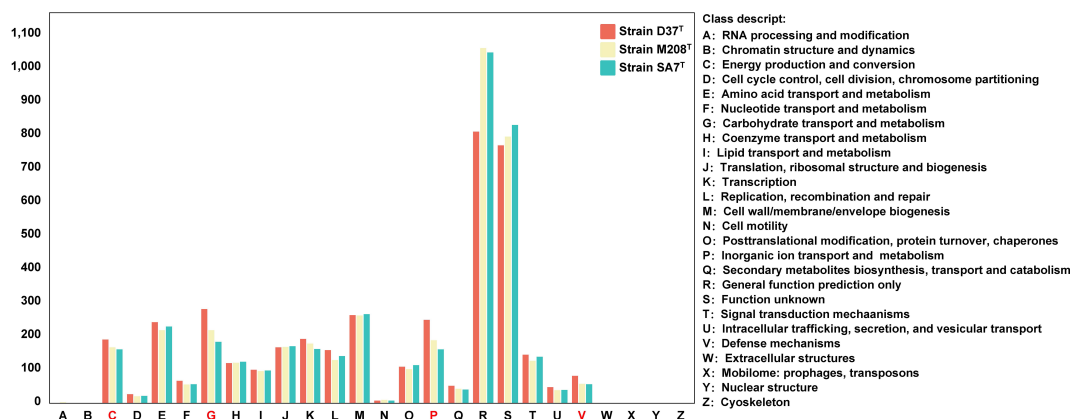


FIGURE 3
The annotation results of clusters of orthologous groups (COG) of the three novel strains. Groups in red means significant differences between three novel strains.

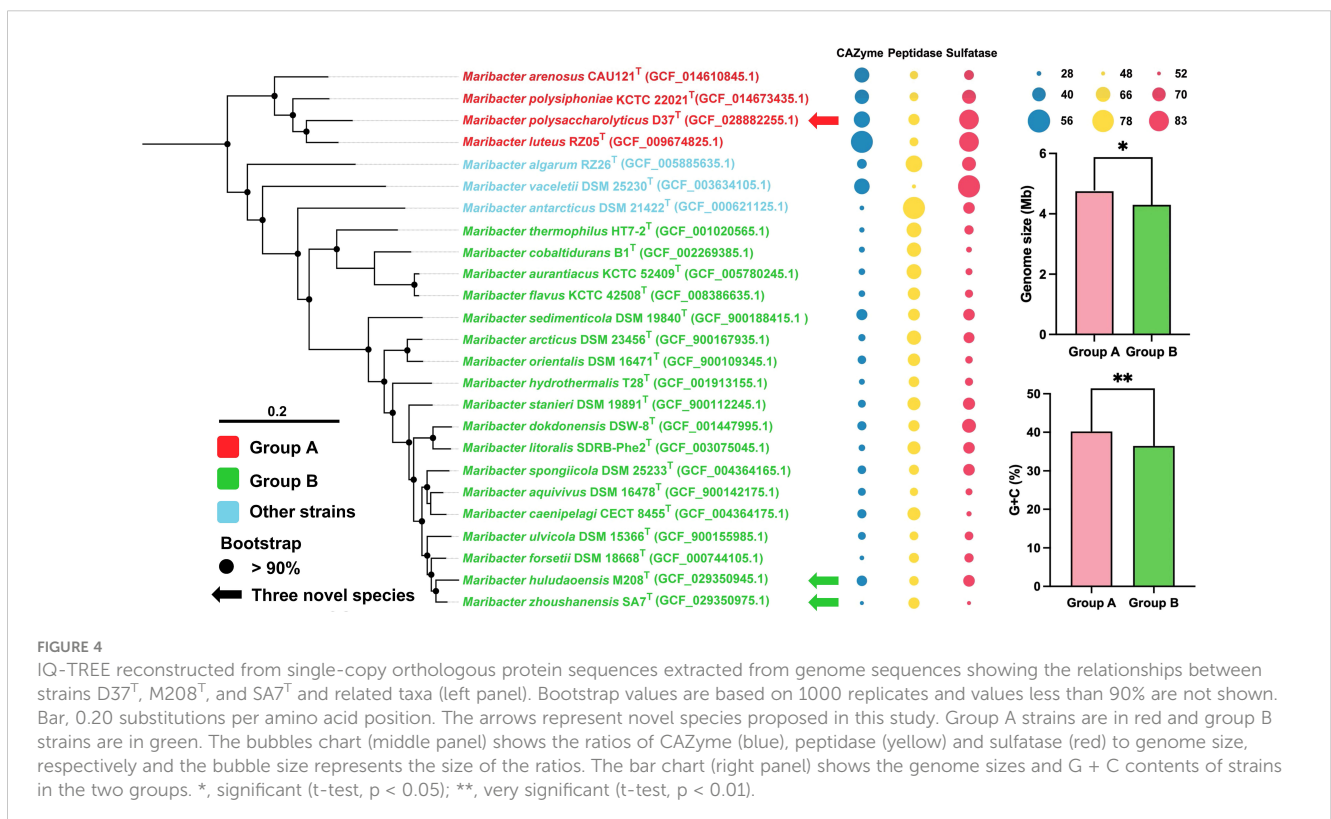
21422^T. The peptidase gene densities of the twenty-five *Maribacter* strains ranged from 48 to 78 per/Mb. Among them, four strains including *M. arenosus* CAU121^T, *M. polysiphoniae* KCTC 22021^T, strain D37^T, and *M. luteus* RZ05^T showed lower peptidase gene densities which were 55, 56, 60, and 56 per/Mb, respectively. The peptidase gene densities of the other eighteen strains ranged from 55 to 66 per/Mb except *M. algarum* RZ26^T, *M. vaceletti* DSM 25230^T, and *M. antarcticus* DSM 21422^T. The sulfatase gene densities of the twenty-five *Maribacter* strains ranged from 52 to 83 per/Mb. Among them, four strains including *M. arenosus* CAU121^T, *M. polysiphoniae* KCTC 22021^T, strain D37^T, *M. luteus* RZ05^T showed higher sulfatase gene densities which were 62, 69, 79, and 79 per/Mb, respectively. The sulfatase gene densities of the other eighteen strains ranged from 52 to 69 per/Mb except *M. algarum* RZ26^T, *M. vaceletti* DSM 25230^T, and *M. antarcticus* DSM 21422^T. According to the above results, the genus *Maribacter* strains were mainly divided into two groups. Four strains (*M. arenosus* CAU121^T, *M. polysiphoniae* KCTC 22021^T, strain D37^T, *M. luteus* RZ05^T) were classified as group A, and except *M. algarum* RZ26^T, *M. vaceletti* DSM 25230^T, and *M. antarcticus* DSM 21422^T which were considered as transition strains, another 18 strains were clustered as group B (Figure 4). The principal component analysis (PCA) based on the number counts of CAZyme and peptidase in the twenty-five *Maribacter* strains supported this classification: all eighteen group B members were clearly clustered together and separated from four group A members (Figure 5) and the phylogenetic trees based on 16S rRNA genes also presented a similar phenomenon, in which four group A strains were clearly set apart from eighteen group B strains

(Figure S9). The average gene densities of CAZyme and sulfatase in group A were higher than group B (48 vs 33 and 72 vs 61 per/Mb, Mann-Whitney *U* test; $p < 0.001$ for CAZyme and $p < 0.05$ for sulfatase). Furthermore, other genome features of these three groups including the genome size and the DNA G + C content also indicated that group A was different from group B (Figure 4). For example, the genome sizes of group B (4.0–4.6 Mb, average 4.3 Mb) were significantly smaller than that of group A (4.2–5.1 Mb, average 4.7 Mb) (t-test, $p < 0.05$). Meanwhile, the DNA G + C contents of group B (34.4%–41.8%, average 36.5%) were also significantly lower than that of group A (38.9%–41.7%, average 40.2%) (t-test, $p < 0.01$).

3.4.2 The composition of CAZyme was different between group A and group B

We further analyzed the composition and distribution of CAZyme after dividing *Maribacter* strains into two groups (Figure 6). Group A had more CAZyme than group B, in particular, group A encoded more GH families than group B (average 134 vs 63; t-test, $p < 0.001$), almost twice as much as group B. But the differences of CAZyme in PL, GT, AA, CE, and CBM were not so significant. The number counts of the CAZyme families including GH3, GH29, GH30, GH43, GH92, and GH130 in group A were significantly higher than group B, and GH76, GH94, and PL8 families were unique in group A. Besides, although the number counts of CAZyme families in group B were less than those in group A, GH74 family only existed in group B.

GH3 family has diverse functions that are usually related to degrading β -glucan in brown algae as exo- β -glucosidase activity



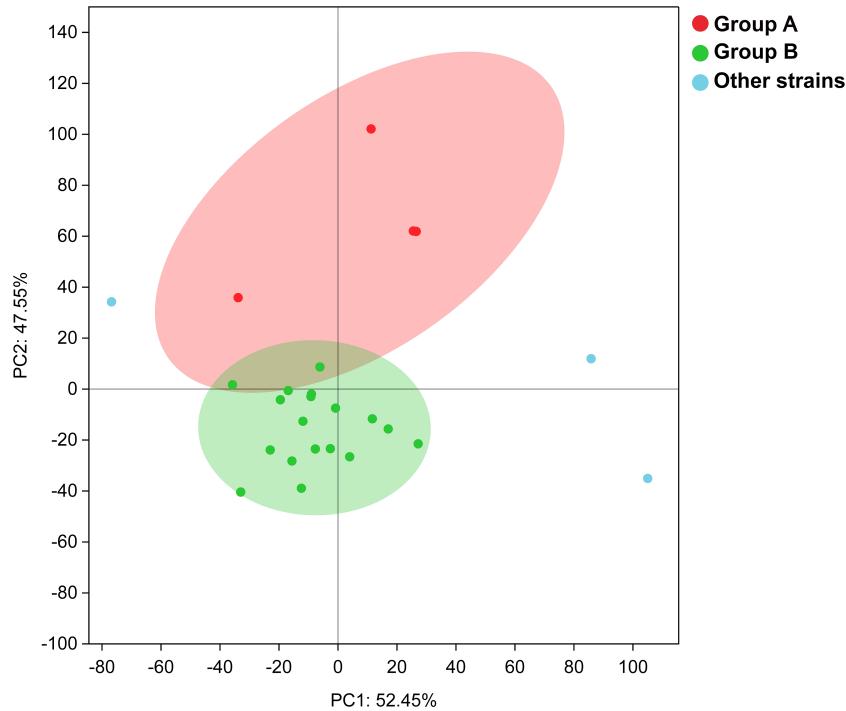


FIGURE 5 The PCA analysis result for the twenty-five *Maribacter* strains based on the number counts of CAZyme and peptidase.

(Tamura et al., 2017). GH3 family usually participates in laminarin degradation with GH17 family which has endo- β -glucosidase activity (Kappelmann et al., 2019). GH29 family mainly showed fucosidase activity and is related to the degradation of fucoidan (Grootaert et al., 2020). GH30 and GH43 families are broader in degradation capacities and both have β -xylosidase activity to degrade xylan, they can be more specific to mixed xylose-containing substrates (Qeshmi et al., 2020). The main function of

GH92 family is exo- α -mannosidases activity (Chen et al., 2018), and it also has an exo-mode of action with mannosidase activities (Zhu et al., 2010; Teeling et al., 2016; Chen et al., 2018). GH130 family is a glycoside phosphorylase, which always degrades mannan with GH26 family (Cuskin et al., 2015). GH76 family shows the activity of endo- α -1,6-mannanase and usually hydrolyzes mannan with GH92 family (Solanki et al., 2022). GH94 family is a glycoside phosphorylase that may work with some other GH families to

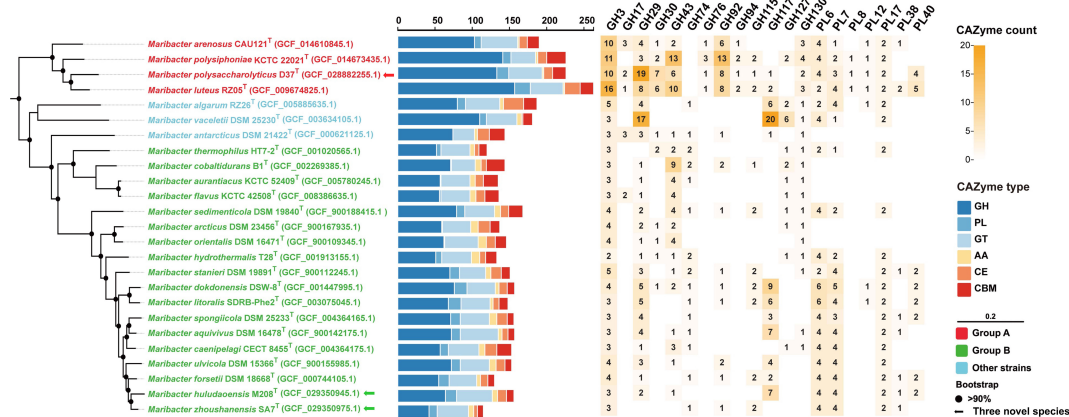


FIGURE 6 The phylogenomic tree based on single-copy orthologous protein sequences showing the relationships between strains D37^T, M208^T, and SA7^T and related taxa (left panel). Bootstrap values are based on 1000 replicates and values less than 90% are not shown. Bar, 0.20 substitutions per amino acid position. The arrows represent novel species proposed in this study. The quantities and categories sum of CAZymes (middle panel) includes GH (dark blue), PL (blue), GT (light blue), AA (yellow), CE (orange), and CBM (red). The numbers and the shade (right panel) means the number counts and relative abundance of selected CAZyme families in twenty-five members of the genus *Maribacter*.

degrade certain oligosaccharides of mannan (Senoura et al., 2011). PL8 family is usually predicted as hyaluronan and chondroitin activities, but it also shows exogenous specificity and synergy which indicates it may be a new type of alginate lyase family (Garron and Cygler, 2014; Pilgaard et al., 2019). Besides, GH74 family is generally considered as xyloglucanase e.g. endo- β -1,4-glucanases (Chen et al., 2022).

3.4.3 The unique PUL in group A is mannan-specific

In *Bacteroidota*, the polysaccharides degradation is usually carried out with distinct PULs. For example, GH92 family is always associated with the degradation of mannan, but the existence of sole GH92 family in the genome cannot fully explain whether it is truly able to degrade mannan. The existence of related PUL can further indicate that a strain has a relatively comprehensive degradation ability for a certain type of substrate. We found the number counts of GH92 family in group A was far higher than group B, and mannan-specific PULs were predicted only in group A strains including *M. arenosus* CAU121^T (1 PUL), *M. polysiphoniae* KCTC 22021^T (3 PULs), strain D37^T (2 PULs), and *M. luteus* RZ05^T (2 PULs), no mannan-specific PUL was found in group B. (Figure 7).

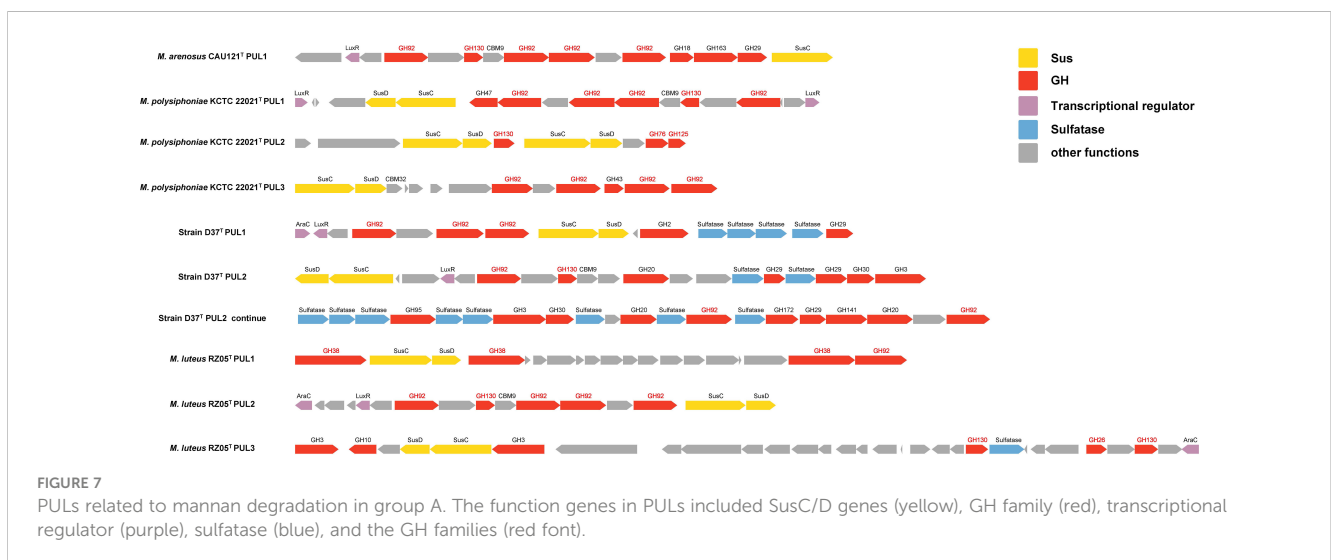
Mannan can be divided into α -mannan and β -mannan. α -mannan has the α -1, 6-D-mannose backbone, and most of the predicted mannan-specific PULs of group A degrade α -mannan, which were shown as three types: (1) PUL consists of transport proteins SusC/D, multiple GH92, one GH130 with certain other GH families, transcriptional regulator *LuxR* but with no sulfatase; the typical PULs were *M. arenosus* CAU121^T PUL1, *M. polysiphoniae* KCTC 22021^T PUL1, and *M. luteus* RZ05^T PUL2; (2) PUL with transport proteins SusC/D, α -mannan related CAZymes which had α -1,6-mannosidases activity or α -mannosidases activity such as GH76, GH125, or GH38; the typical PULs were *M. polysiphoniae* KCTC 22021^T PUL2, and *M. luteus* RZ05^T PUL1; (3) PUL contains transport proteins SusC/D,

multiple GH92 with several other GH families, transcriptional regulator *LuxR* and abundant sulfatases; the typical PULs were PUL1 and PUL2 in strain D37^T. β -mannan contains β -1, 4-linked backbone with mannose as the major component, only one type of β -mannan-specific PUL was predicted in group A, which contained transport proteins SusC/D, GH130, and GH26 (endo- β -1,4-mannanases activity). The typical PUL was *M. luteus* RZ05^T PUL3.

3.4.4 The differences between group A and group B indicate their different niches

Marine bacteria exist in distinct environments, while marine *Bacteroidota* is considered to have two types of existing modes (Fernández-Gómez et al., 2013). For instance, marine *Bacteroidota* emerges as important responders during algal blooms, many of them exhibit a significant portion of macroalgae-related representatives (Kruger et al., 2019). The number of *Polaribacter* strains are associated with algae degradation, it has shown a significant increase during North Sea algal blooms (Avci et al., 2020). Besides marine *Bacteroidota*, certain marine heterotrophic bacteria also have evolved the capability to thrive on algal polysaccharides, such as *Pseudoalteromonas* strains which are mainly isolated from red algae, the analysis of the genomes of these strains revealed a high abundance of carbohydrate-active enzymes (Gobet et al., 2018). Meanwhile, marine flavobacterium *Dokdonia donghaensis* MED134^T prefers low-nutrition environments and possesses a small genome size, and it encodes more peptidase rather than CAZyme for growth through genome analysis, which reveals that this strain has few potentials for degrading algal polysaccharides (Gonzalez et al., 2011). The genome analysis for *Polaribacter* sp. MED152 reveals multitudinous presence genes associated with motility and proteorhodopsin, and these genetic traits potentially contribute to its ability to thrive in nutrient-poor marine surface environments (Gonzalez et al., 2008).

The ratio of CAZyme combined with peptidase can be utilized for niche assessment (Fernández-Gómez et al., 2013; Mann et al., 2013;



Unfried et al., 2018). The high proportion of CAZyme and low proportion of peptidase are considered to be a “particle-associated” mode of existence, and the abundant presence of peptidase in the genome is considered to be one of the indicators for a “free-living” mode of existence (Gonzalez et al., 2011; Fernández-Gómez et al., 2013; Xing et al., 2015; Xue et al., 2020). Some marine bacteria contain certain numbers of CAZymes (not in high proportion) in the genome, and they may also prefer an oligotrophic marine environment and “free-living” mode (Xu et al., 2015; Arnosti et al., 2021). In addition, the algal polysaccharides are the primary constituent of the cell wall in marine algae and encompass a wide range of sulfated polysaccharides such as fucoidan, carrageenan and ulvan (Ramanan et al., 2016; Hentati et al., 2020). The abundant presence of sulfatase in the genome can also reflect the preference of strains to algal abundant environments. Our study found the gene densities of CAZyme and sulfatase in group A were high, while the gene densities of peptidase were relatively low. On the contrary, group B possessed higher gene densities of peptidase than CAZyme and sulfatase. Nevertheless, smaller genomes may enhance the adaptability of strains to oligotrophic marine environments (Qin et al., 2019; Liang et al., 2022). A smaller genome may be an adaptation strategy to reduce costs in microbial DNA replication, and the lower DNA G + C content can reduce the energy consumption in the process of bacterial replication in the oligotrophic environment (Luo and Moran, 2015). As a result, particle-associated bacteria prefer to have larger genome sizes than free-living bacteria which are usually found in oligotrophic environments (Luo et al., 2014). Our results indicate that the genome size and the DNA G + C content of group A are much higher than those of group B. Therefore, through the average gene densities of CAZyme, peptidase and sulfatase, and other genomic features, we propose that two groups may have different niche adaptation strategies to different marine environments. Group A can be assigned as the “particle-associated” mode of existence, while group B is the “free-living” mode of existence.

We further analyzed the detailed profiles of CAZyme in different groups. The results show that group A had more CAZyme than group B whether in total number count or diversity, including GH3, GH29, GH30, GH43, GH92, and GH130 families, which are related to the degradation of laminarin, fucoidan, mannan, xylose, and xylan, respectively. This phenomenon is similar to other algae-associated paradigms observed in other well-studied marine flavobacteria strains in the genus *Gramellai* and *Polaribacter* (Kabisch et al., 2014; Xing et al., 2015). Furthermore, mannan mainly comes from various algae, including red and green algae. For example, sulfated α -1,3-linked D-mannan is found in red alga *Nothogenia fastigiata* (Kolender et al., 1997) and mixed-linkage mannan exists in green alga *Codium fragile* (Tabarsa et al., 2013). GH92 family is considered as the specific CAZyme related to mannan degradation and widely occurs in *Flavobacteriaceae* (Teeling et al., 2012; Zeugner et al., 2021). Our research also showed that GH92 family was abundant in group A and the mannan-specific PUL only appeared in this group. This can be further evidence for the proposed “particle-associated” mode of existence of group A.

4 Conclusions

Phenotypic and genotypic characterization analysis of strains D37^T, M208^T, and SA7^T in this study shows unequivocally that the three strains should be assigned as novel species of the genus *Maribacter*, for which the names are proposed as *Maribacter polysaccharolyticus* sp. nov., *Maribacter huludaoensis* sp. nov., and *Maribacter zhoushanensis* sp. nov., respectively. Furthermore, we compared all available genomes of *Maribacter* representatives and determined that they could be divided into two groups (A and B). Two groups are different in gene densities of CAZyme, peptidase and sulfatase, genome size and G + C content. Group A possesses more CAZymes and sulfatases than group B, especially in GH families including GH3, GH29, GH30, GH43, GH92, and GH130 which are related to degrading laminarin, fucoidan, mannan, xylose, and xylan, respectively. In addition, mannan-specific PUL is only found in group A. These results indicate that two groups have different niche adaptation strategies, and we consider that group A uses the “particle-associated” strategy of existence and prefers the niche in environments with enriched marine polysaccharides, while group B uses the “free-living” strategy of existence and prefers the niche in oligotrophic marine.

4.1 Description of *Maribacter polysaccharolyticus* sp. Nov.

Maribacter polysaccharolyticus (po.ly.sac.cha.ro.ly'ti.cus. Gr. Masc. adj. *polys*, many; Gr. Neut. N. *sakcharon*, sugar; Gr. Masc. adj. *lytikos*, dissolving; N.L. masc. adj. *polysaccharolyticus*, many sugars dissolving).

Cells are Gram-stain-negative, strictly aerobic, non-motile, oxidase-positive and catalase-positive. Cells are rod-shaped with 1.8-3.3 μ m in length and 0.6-0.8 μ m in width. Colonies are orange, 1-2mm in diameter, round, opaque, border smooth, and convex. Growth can be observed at 15-37 °C (optimum, 28 °C), pH 5.5-8.5 (optimum, pH 7.0), and with 0-6% (w/v) NaCl (optimum, 2.0-3.5%). In the API 20NE test, cells were positive for reduction of nitrate to nitrite, fermentation of glucose, hydrolyzation of esculin and β -galactosidase. In the API ZYM test, alkaline phosphatase, leucine arylamidase, valine arylamidase, trypsin, acid phosphatase, naphthol-AS-BI-phosphorylase, and N-acetyl- β -glucosaminidase are positive. esterase (C4), esterase lipase (C8), cysteine arylamidase, chymotrypsin, and β -fucosidase are weak. Acid is produced from glycerol, D-arabinose, D-xylose, D-galactose, D-glucose, D-fructose, D-mannose, D-mannitol, methyl- α D-mannopyranoside, methyl- α D-glucopyranoside, N-acetyl-glucosamine, amygdalin, arbutin, esculin ferric citrate, salicin, D-cellobiose, D-maltose, D-lactose, D-melibiose, D-saccharose, D-trehalose, inulin, D-melezitose, D-raffinose, starch, glycogen, xylitol, gentiobiose, D-turanose, L-fucose, and potassium 2-ketogluconate. The major fatty acids (>10%) are iso-C_{15:0} and iso-C_{17:0} 3-OH. The major respiratory quinone is MK-6. The major polar lipids contain phosphatidylethanolamine, two unidentified glycolipids, one unidentified aminolipid, and three unidentified lipids. The G+C content based on the genome sequence is 41.7%.

The strain D37^T (=MCCC 1K06123^T =KCTC 82772^T) was isolated from an intertidal sediment sample collected from Zhoushan, Zhejiang, PR China (21°35' N, 109°9' E). The GenBank accession numbers for the 16S rRNA gene and genome sequences of strain D37^T are OP132875 and GCF_014610845.1, respectively.

4.2 Description of *Maribacter huludaoensis* sp. nov.

Maribacter huludaoensis (hu.lu.dao.en'sis. N.L. masc./fem. adj. *huludaoensis*, pertaining to Huludao, PR China, where the strain was isolated).

Cells are Gram-stain-negative, strictly aerobic, non-motile, oxidase-weakly, and catalase-negative. Cells are rod-shaped with 1.7-2.7 μm in length and 0.3-0.4 μm in width. Colonies are orange, 1-2mm in diameter, round, opaque, border smooth and convex. Growth can be observed at 4-35°C (optimum, 28°C), pH 6.0-8.5 (optimum, pH 6.5) and with 0.5-6.0% (w/v) NaCl (optimum, 1.5-2.5%). Cellulose, tyrosine, Tween 20, 40, 60, and 80 are hydrolyzed, but starch and casein are not hydrolyzed. In the API 20NE test, cells were positive for reduction of nitrate to nitrite, hydrolyzation of esculin and β-galactosidase. In the API ZYM test, alkaline phosphatase, leucine arylamidase, valine arylamidase, chymotrypsin, acid phosphatase, naphthol-AS-BI-phosphorylase, β-galactosidase, α-glucosidase, and N-acetyl-β-glucosaminidase are positive. Esterase (C4), esterase lipase (C8), cysteine arylamidase, trypsin, α-galactosidase, β-fucosidase, and α-mannosidase are weak. Acid is produced from D-xylose, methyl-βD-xylopyranoside (weakly), D-galactose, D-glucose, D-fructose (weakly), D-mannose (weakly), L-rhamnose, methyl-αD-mannopyranoside (weakly), methyl-αD-glucopyranoside, N-acetyl-glucosamine (weakly), amygdalin, arbutin, esculin ferric citrate, salicin, D-cellobiose, D-maltose, D-lactose, D-melibiose, D-saccharose, D-trehalose, inulin (weakly), D-melezitose (weakly), D-raffinose, gentiobiose, D-turanose, and potassium gluconate. The major fatty acids (>10%) are iso-C_{15:0}, iso-C_{17:0} 3-OH, Summed Feature 1, and Summed Feature 3. The major respiratory quinone is MK-6. The major polar lipids comprise phosphatidylethanolamine, two unidentified glycolipids, one unidentified aminolipid, and two unidentified lipids. The G+C content based on the genome sequence is 35.9%.

The strain M208^T (=MCCC 1K08510^T =KCTC 82763^T) is an intertidal sediment sample taken from the coastal zone of Huludao, Liaoning, PR China (40°41' N, 120°56' E). The GenBank accession numbers for the 16S rRNA gene and genome sequences of strain M208^T are OQ165154 and GCF_029350945.1, respectively.

4.3 Description of *Maribacter zhoushanensis* sp. nov.

Maribacter zhoushanensis (zhou.shan.en'sis. N.L. masc./fem. adj. *zhoushanense*, pertaining to Zhoushan, eastern China, where the strain was isolated)

Cells are Gram-stain-negative, strictly aerobic, non-motile, oxidase-weakly, and catalase-negative. Cells are rod-shaped with 1.5-3 μm in length and 0.6-0.8 μm in width. Colonies are orange, 0.5-1mm in diameter, round, opaque, border smooth, and convex. Growth can be observed at 4-30°C (optimum, 25°C), pH 5.5-9.0 (optimum, pH 7.0), and with 0.5-6.0% (w/v) NaCl (optimum, 1-3%). Cellulose, tyrosine, Tween 20, 40, 60, and 80 are hydrolyzed, but starch and casein are not hydrolyzed. In the API 20NE test, cells were positive for reduction of nitrate to nitrite, hydrolyzation of esculin and β-galactosidase. In the API ZYM test, alkaline phosphatase, esterase (C4), esterase lipase (C8), leucine arylamidase, valine arylamidase, acid phosphatase, naphthol-AS-BI-phosphorylase, α-glucosidase, and N-acetyl-β-glucosaminidase are positive. Chymotrypsin, α-galactosidase and α-mannosidase are weak. Acid is produced from D-xylose, methyl-βD-xylopyranoside (weakly), D-galactose, D-glucose, D-fructose, D-mannose, D-mannitol, methyl-αD-mannopyranoside (weakly), methyl-αD-glucopyranoside, N-acetyl-glucosamine, amygdalin, arbutin, esculin ferric citrate, salicin, D-cellobiose, D-maltose, D-lactose, D-melibiose, D-saccharose, D-trehalose, inulin (weakly), D-melezitose (weakly), D-raffinose, starch, glycogen (weakly), xylitol (weakly), gentiobiose, D-turanose, potassium gluconate, and potassium 2-ketogluconate. The major fatty acids (>10%) are iso-C_{15:0}, iso-C_{17:0} 3-OH, and Summed feature 1. The major respiratory quinone is MK-6. The major polar lipids consist of phosphatidylethanolamine, three unidentified glycolipids, one unidentified aminolipid, and three unidentified lipids. The G+C content based on the genome sequence is 34.8%.

The strain SA7^T (=MCCC 1K08511^T =KCTC 82773^T) was isolated from an intertidal sediment sample collected from Zhoushan, Zhejiang, PR China (21°35' N, 109°9' E). The GenBank accession numbers for the 16S rRNA gene and genome sequences of strain SA7^T are OQ165151 and GCF_029350975.1, respectively.

Data availability statement

The original contributions presented in the study are publicly available. This data can be found here: <https://www.ncbi.nlm.nih.gov/>, accession number: OP132875, OQ165154, OQ165151, JARBUR000000000, JARKMS000000000 and JARKMR000000000.

Author contributions

J-WG and HD collected the samples and isolated these strains. J-WG, J-JY, W-JL, and D-YH performed data collection and analysis. J-WG and CS wrote the manuscript. LX and CS performed project guidance and critical revision of manuscripts. All authors contributed to the article and approved the submitted version.

Funding

This study was supported by National Science and Technology Fundamental Resources Investigation Program of China

(2019FY100700), Zhejiang Provincial Natural Science Foundation of China (LDT23D06025D06), the Key R&D Program of Zhejiang (#2023C03011), National Natural Science Foundation of China (No. 31900003), and the Fundamental Research Funds of Zhejiang Sci-Tech University (22042315-Y).

Conflict of interest

Authors J-WG, J-JY, W-JL, LX, and CS are employed by Shaoxing Biomedical Research Institute of Zhejiang Sci-Tech University Co., Ltd.

The remaining authors declare that the research was conducted in the absence of any commercial or financial relationships that could be construed as a potential conflict of interest.

References

- Arnosti, C., Wietz, M., Brinkhoff, T., Hehemann, J. H., Probandt, D., Zeugner, L., et al. (2021). The biogeochemistry of marine polysaccharides: sources, inventories, and bacterial drivers of the carbohydrate cycle. *Ann. Rev. Mar. Sci.* 13, 81–108. doi: 10.1146/annurev-marine-032020-012810
- Avcı, B., Kruger, K., Fuchs, B. M., Teeling, H., and Amann, R. I. (2020). Polysaccharide niche partitioning of distinct *Polaribacter* clades during North Sea spring algal blooms. *ISME J.* 14, 1369–1383. doi: 10.1038/s41396-020-0601-y
- Aziz, R. K., Bartels, D., Best, A. A., DeJongh, M., Disz, T., Edwards, R. A., et al. (2008). The RAST Server: rapid annotations using subsystems technology. *BMC Genomics* 75, 1–15. doi: 10.1186/1471-2164-9-75
- Barbeyron, T., Carpentier, F., L'Haridon, S., Schuler, M., Michel, G., and Amann, R. (2008). Description of *Maribacter forsetii* sp. nov., a marine *Flavobacteriaceae* isolated from North Sea water, and emended description of the genus *Maribacter*. *Int. J. Syst. Evol. Microbiol.* 58, 790–797. doi: 10.1099/ijs.0.65469-0
- Barbeyron, T., Thomas, F., Barbe, V., Teeling, H., Schenowitz, C., Dossat, C., et al. (2016). Habitat and taxon as driving forces of carbohydrate catabolism in marine heterotrophic bacteria: example of the model algae-associated bacterium *Zobellia galactanivorans* Dsj(T). *Environ. Microbiol.* 18, 4610–4627. doi: 10.1111/1462-2920.13584
- Bartlau, N., Wichels, A., Krohne, G., Adriaenssens, E. M., Heins, A., Fuchs, B. M., et al. (2022). Highly diverse flavobacterial phages isolated from North Sea spring blooms. *ISME J.* 16, 555–568. doi: 10.1038/s41396-021-01097-4
- Bennke, C. M., Kruger, K., Kappelmann, L., Huang, S., Gobet, A., Schuler, M., et al. (2016). Polysaccharide utilisation loci of Bacteroidetes from two contrasting open ocean sites in the North Atlantic. *Environ. Microbiol.* 18, 4456–4470. doi: 10.1111/1462-2920.13429
- Cantalapiedra, C. P., Hernandez-Plaza, A., Letunic, I., Bork, P., and Huerta-Cepas, J. (2021). eggNOG-mapper v2: Functional Annotation, Orthology Assignments, and Domain Prediction at the Metagenomic Scale. *Mol. Biol. Evol.* 38, 5825–5829. doi: 10.1093/molbev/msab293
- Capella-Gutierrez, S., Silla-Martinez, J. M., and Gabaldon, T. (2009). trimAl: a tool for automated alignment trimming in large-scale phylogenetic analyses. *Bioinformatics* 25, 1972–1973. doi: 10.1093/bioinformatics/btp348
- Chen, J., Robb, C. S., Unfried, F., Kappelmann, L., Markert, S., Song, T., et al. (2018). Alpha- and beta-mannan utilization by marine Bacteroidetes. *Environ. Microbiol.* 20, 4127–4140. doi: 10.1111/1462-2920.14414
- Chen, M., Ropartz, D., Mac-Bear, J., Bonnin, E., and Lahaye, M. (2022). New insight into the mode of action of a GH74 xyloglucanase on tamarind seed xyloglucan: Action pattern and cleavage site. *Carbohydr. Res.* 521, 108661. doi: 10.1016/j.carres.2022.108661
- Chun, J., Oren, A., Ventosa, A., Christensen, H., Arahall, D. R., da Costa, M. S., et al. (2018). Proposed minimal standards for the use of genome data for the taxonomy of prokaryotes. *Int. J. Syst. Evol. Microbiol.* 68, 461–466. doi: 10.1099/ijssem.0.002516
- Cuskin, F., Basle, A., Ladeveze, S., Day, A. M., Gilbert, H. J., Davies, G. J., et al. (2015). The GH130 family of mannoside phosphorylases contains glycoside hydrolases that target beta-1,2-mannosidic linkages in candida mannan. *J. Biol. Chem.* 290, 25023–25033. doi: 10.1074/jbc.M115.681460
- Do, K.-A. (1992). A simulation study of balanced and antithetic bootstrap resampling methods. *J. Stat. Comput. Simulation* 40, 153–166. doi: 10.1080/00949659208811373
- Fang, C., Wu, Y. H., Xamxid, M., Wang, C. S., and Xu, X. W. (2017). *Maribacter cobaltidurans* sp. nov., a heavy-metal-tolerant bacterium isolated from deep-sea sediment. *Int. J. Syst. Evol. Microbiol.* 67, 5261–5267. doi: 10.1099/ijssem.0.002458
- Felsenstein, J. (1981). Evolutionary trees from DNA sequences: a maximum likelihood approach. *J. Mol. Evol.* 17, 368–376. doi: 10.1007/bf01734359
- Fernández-Gómez, B., Richter, M., Schüler, M., Pinhassi, J., Acinas, S. G., González, J. M., et al. (2013). Ecology of marine Bacteroidetes: a comparative genomics approach. *ISME J.* 7, 1026–1037. doi: 10.1038/ismej.2012.169
- Ficko-Blean, E., Prechoux, A., Thomas, F., Rochat, T., Larocque, R., Zhu, Y., et al. (2017). Carrageenan catabolism is encoded by a complex regulon in marine heterotrophic bacteria. *Nat. Commun.* 8, 1685. doi: 10.1038/s41467-017-01832-6
- Fitch, W. M. (1971). Toward defining the course of evolution: minimum change for a specific tree topology. *Systematic Biol.* 20, 406–416. doi: 10.1093/sysbio/20.4.406
- Gao, J. W., He, D. Y., Zhang, W. W., Wang, Y. R., Su, Y., Ying, J. J., et al. (2023). *Aestuariabaculum lutulentum* sp. nov., a marine bacterium isolated from coastal sediment in Beihai. *Arch. Microbiol.* 187, 205. doi: 10.1007/s00203-023-03535-7
- Garron, M. L., and Cygler, M. (2014). Uronic polysaccharide degrading enzymes. *Curr. Opin. Struct. Biol.* 28, 87–95. doi: 10.1016/j.sbi.2014.07.012
- Gavriliidou, A., Gutleben, J., Versluis, D., Forgiarini, F., van Passel, M. W. J., Ingham, C. J., et al. (2020). Comparative genomic analysis of *Flavobacteriaceae*: insights into carbohydrate metabolism, gliding motility and secondary metabolite biosynthesis. *BMC Genomics* 569, 1–21. doi: 10.1186/s12864-020-06971-7
- Gobet, A., Barbeyron, T., Matarid-Mann, M., Magdelenat, G., Vallent, D., Duchaud, E., et al. (2018). Evolutionary evidence of algal polysaccharide degradation acquisition by *Pseudoalteromonas carrageenovora* 9(T) to adapt to macroalgal niches. *Front. Microbiol.* 9, 2740. doi: 10.3389/fmicb.2018.02740
- Gonzalez, J. M., Fernandez-Gomez, B., Fernandez-Guerra, A., Gomez-Consarnau, L., Sanchez, O., Coll-Llado, M., et al. (2008). Genome analysis of the proteorhodopsin-containing marine bacterium *Polaribacter* sp. MED152 (*Flavobacterium*). *Proc. Natl. Acad. Sci. U.S.A.* 105, 8724–8729. doi: 10.1073/pnas.0712027105
- Gonzalez, J. M., Pinhassi, J., Fernandez-Gomez, B., Coll-Llado, M., Gonzalez-Velazquez, M., Puigbo, P., et al. (2011). Genomics of the proteorhodopsin-containing marine flavobacterium *Dokdonia* sp. strain MED134. *Appl. Environ. Microbiol.* 77, 8676–8686. doi: 10.1128/AEM.06152-11
- Grotaert, H., Van Landuyt, L., Hulpiau, P., and Callewaert, N. (2020). Functional exploration of the GH29 fucosidase family. *Glycobiology* 30, 735–745. doi: 10.1093/glycob/cwaa023
- Hentati, F., Tounsi, L., Djomdi, D., Pierre, G., Delattre, C., Ursu, A. V., et al. (2020). Bioactive polysaccharides from seaweeds. *Molecules* 25, 3152. doi: 10.3390/molecules25143152
- Jackson, S. A., Kennedy, J., Morrissey, J. P., O'Gara, F., and Dobson, A. D. W. (2015). *Maribacter spongiicola* sp. nov. and *Maribacter vacelletii* sp. nov., isolated from marine sponges, and emended description of the genus *Maribacter*. *Int. J. Syst. Evol. Microbiol.* 65, 2097–2103. doi: 10.1099/ijs.0.000224
- Jin, M., Kim, M., Kim, J. Y., Song, H. S., Cha, I. T., Roh, S. W., et al. (2017). *Maribacter pelagius* sp. nov., isolated from seawater. *Int. J. Syst. Evol. Microbiol.* 67, 3834–3839. doi: 10.1099/ijssem.0.002203
- Jung, Y. T., Lee, J. S., and Yoon, J. H. (2014). *Maribacter caenipelagi* sp. nov., a member of the *Flavobacteriaceae* isolated from a tidal flat sediment of the Yellow Sea in Korea. *Antonie Van Leeuwenhoek* 106, 733–742. doi: 10.1007/s10482-014-0243-z

Publisher's note

All claims expressed in this article are solely those of the authors and do not necessarily represent those of their affiliated organizations, or those of the publisher, the editors and the reviewers. Any product that may be evaluated in this article, or claim that may be made by its manufacturer, is not guaranteed or endorsed by the publisher.

Supplementary material

The Supplementary Material for this article can be found online at: <https://www.frontiersin.org/articles/10.3389/fmars.2023.1248754/full#supplementary-material>

- Kabisch, A., Otto, A., König, S., Becher, D., Albrecht, D., Schuler, M., et al. (2014). Functional characterization of polysaccharide utilization loci in the marine Bacteroidetes *Gramella forsetii* KT0803. *ISME J.* 8, 1492–1502. doi: 10.1038/ismej.2014.4
- Kanehisa, M., Furumichi, M., Tanabe, M., Sato, Y., and Morishima, K. (2017). KEGG: new perspectives on genomes, pathways, diseases and drugs. *Nucleic Acids Res.* 45, D353–D361. doi: 10.1093/nar/gkw1092
- Kang, H., Cha, I., Kim, H., and Joh, K. (2018). *Maribacter maritimus* sp. nov., isolated from seawater. *Int. J. Syst. Evol. Microbiol.* 68, 2431–2436. doi: 10.1099/ijsem.0.002843
- Kappelmann, L., Kruger, K., Hehemann, J. H., Harder, J., Markert, S., Unfried, F., et al. (2019). Polysaccharide utilization loci of North Sea Flavobacteriia as basis for using SusC/D-protein expression for predicting major phytoplankton glycans. *ISME J.* 13, 76–91. doi: 10.1038/s41396-018-0242-6
- Katoh, K., and Standley, D. M. (2013). MAFFT multiple sequence alignment software version 7: improvements in performance and usability. *Mol. Biol. Evol.* 30, 772–780. doi: 10.1093/molbev/mst010
- Khan, S. A., Jeong, S. E., Baek, J. H., and Jeon, C. O. (2020). *Maribacter algicola* sp. nov., isolated from a marine red alga, *Porphyridium marinum*, and transfer of *Maripseudobacter aurantiacus* Chen et al. 2017 to the genus *Maribacter* as *Maribacter aurantiacus* comb. nov. *Int. J. Syst. Evol. Microbiol.* 70, 797–804. doi: 10.1099/ijsem.0.003828
- Kim, M., Oh, H.-S., Park, S.-C., and Chun, J. (2014). Towards a taxonomic coherence between average nucleotide identity and 16S rRNA gene sequence similarity for species demarcation of prokaryotes. *Int. J. Systematic Evolutionary Microbiol.* 64, 346–351. doi: 10.1099/ijse.0.059774-0
- Kimura, M. (1980). A simple method for estimating evolutionary rates of base substitutions through comparative studies of nucleotide sequences. *J. Mol. Evol.* 16, 111–120. doi: 10.1007/bf01731581
- Klippel, B., Lochner, A., Bruce, D. C., Davenport, K. W., Detter, C., Goodwin, L. A., et al. (2011). Complete genome sequences of *Krokinobacter* sp. strain 4H-3-7-5 and *Lacinutrix* sp. strain 5H-3-7-4, polysaccharide-degrading members of the family *Flavobacteriaceae*. *J. Bacteriol.* 193, 4545–4546. doi: 10.1128/JB.05518-11
- Kolender, A. A., Pujol, C. A., Damonte, E. B., Matulewicz, M. C., and Cerezo, A. S. (1997). The system of sulfated alpha-(1->3)-linked D-mannans from the red seaweed *Notogentia fastigiata*: structures, antihyperic and anticoagulant properties. *Carbohydr. Res.* 304, 53–60. doi: 10.1016/S0008-6215(97)00201-2
- Kruger, K., Chafee, M., Ben Francis, T., Glavina Del Rio, T., Becher, D., Schweder, T., et al. (2019). In marine Bacteroidetes the bulk of glycan degradation during algae blooms is mediated by few clades using a restricted set of genes. *ISME J.* 13, 2800–2816. doi: 10.1038/s41396-019-0476-y
- Lagesen, K., Hallin, P., Rodland, E. A., Staerfeldt, H. H., Rognes, T., and Ussery, D. W. (2007). RNAmmer: consistent and robust annotation of ribosomal RNA genes. *Nucleic Acids Res.* 35, 3100–3108. doi: 10.1093/nar/gkm160
- Lee, I., Ouk Kim, Y., Park, S. C., and Chun, J. (2016). OrthoANI: An improved algorithm and software for calculating average nucleotide identity. *Int. J. Syst. Evol. Microbiol.* 66, 1100–1103. doi: 10.1099/ijsem.0.000760
- Liang, J. C., Liu, J. W., Wang, X. L., Sun, H., Zhang, Y. L., Ju, F., et al. (2022). Genomic analysis reveals adaptation of *Vibrio campbellii* to the hadal ocean? *Appl. Environ. Microbiol.* 88, 00575–22. doi: 10.1128/aem.00575-22
- Liu, A., Zhang, Y. J., Liu, D. K., and Li, X. Z. (2020). *Maribacter luteus* sp. nov., a marine bacterium isolated from intertidal sand of the Yellow Sea. *Int. J. Syst. Evol. Microbiol.* 70, 3497–3503. doi: 10.1099/ijsem.0.004206
- Lo, N., Jin, H. M., and Jeon, C. O. (2013). *Maribacter aestuarii* sp. nov., isolated from tidal flat sediment, and an emended description of the genus *Maribacter*. *Int. J. Syst. Evol. Microbiol.* 63, 3409–3414. doi: 10.1099/ijse.0.050054-0
- Luo, H., and Moran, M. A. (2015). How do divergent ecological strategies emerge among marine bacterioplankton lineages? *Trends Microbiol.* 23, 577–584. doi: 10.1016/j.tim.2015.05.004
- Luo, H., Swan, B. K., Stepanauskas, R., Hughes, A. L., and Moran, M. A. (2014). Evolutionary analysis of a streamlined lineage of surface ocean Roseobacters. *ISME J.* 8, 1428–1439. doi: 10.1038/ismej.2013.248
- Mann, A. J., Hahnke, R. L., Huang, S., Werner, J., Xing, P., Barbeyron, T., et al. (2013). The genome of the alga-associated marine flavobacterium *Formosa agariphila* KMM 3901T reveals a broad potential for degradation of algal polysaccharides. *Appl. Environ. Microbiol.* 79, 6813–6822. doi: 10.1128/AEM.01937-13
- Meier-Kolthoff, J. P., Auch, A. F., Klenk, H. P., and Goker, M. (2013). Genome sequence-based species delimitation with confidence intervals and improved distance functions. *BMC Bioinf.* 14, 1–14. doi: 10.1186/1471-2105-14-60
- Nedashkovskaya, O. I., Kim, S. B., Han, S. K., Lysenko, A. M., Rohde, M., Rhee, M. S., et al. (2004). *Maribacter* gen. nov., a new member of the family *Flavobacteriaceae*, isolated from marine habitats, containing the species *Maribacter sedimenticola* sp. nov., *Maribacter aquivivus* sp. nov., *Maribacter orientalis* sp. nov. and *Maribacter ulvicola* sp. nov. *Int. J. Syst. Evol. Microbiol.* 54, 1017–1023. doi: 10.1099/ijse.0.02849-0
- Nedashkovskaya, O. I., Kim, S. B., and Mikhailov, V. V. (2010). *Maribacter stanieri* sp. nov., a marine bacterium of the family *Flavobacteriaceae*. *Int. J. Syst. Evol. Microbiol.* 60, 214–218. doi: 10.1099/ijse.0.012286-0
- Nedashkovskaya, O. I., Vancanneyt, M., De Vos, P., Kim, S. B., Lee, M. S., and Mikhailov, V. V. (2007). *Maribacter polysiphoniae* sp. nov., isolated from a red alga. *Int. J. Syst. Evol. Microbiol.* 57, 2840–2843. doi: 10.1099/ijse.0.065181-0
- Niu, L., Xie, X., Li, Y., Hu, Q., Wang, C., Zhang, W., et al. (2022). Effects of nitrogen on the longitudinal and vertical patterns of the composition and potential function of bacterial and archaeal communities in the tidal mudflats. *Sci. Total Environ.* 806, 151210. doi: 10.1016/j.scitotenv.2021.151210
- Park, S., Jung, Y. T., Won, S. M., and Yoon, J. H. (2016). *Maribacter litorisediminis* sp. nov., isolated from a tidal flat. *Int. J. Syst. Evol. Microbiol.* 66, 4236–4242. doi: 10.1099/ijsem.0.001341
- Parks, D. H., Imelfort, M., Skennerton, C. T., Hugenholtz, P., and Tyson, G. W. (2015). CheckM: assessing the quality of microbial genomes recovered from isolates, single cells, and metagenomes. *Genome Res.* 25, 1043–1055. doi: 10.1101/gr.186072.114
- Pilgaard, B., Wilkens, C., Herbst, F. A., Vuillemin, M., Rhein-Knudsen, N., Meyer, A. S., et al. (2019). Proteomic enzyme analysis of the marine fungus *Paradendryphiella salina* reveals alginate lyase as a minimal adaptation strategy for brown algae degradation. *Sci. Rep.* 9, 12338. doi: 10.1038/s41598-019-48823-9
- Qeshmi, F. I., Homaei, A., Fernandes, P., Hemmati, R., Dijkstra, B. W., and Khajeh, K. (2020). Xylanases from marine microorganisms: A brief overview on scope, sources, features and potential applications. *Biochim. Biophys. Acta Proteins Proteom* 1868, 140312. doi: 10.1016/j.bbapap.2019.140312
- Qin, Q. L., Li, Y., Sun, L. L., Wang, Z. B., Wang, S., Chen, X. L., et al. (2019). Trophic specialization results in genomic reduction in free-living marine idiominaria bacteria. *Mbio.* 10, 02545–18. doi: 10.1128/mBio.02545-18
- Ramanan, R., Kim, B. H., Cho, D. H., Oh, H. M., and Kim, H. S. (2016). Algae-bacteria interactions: Evolution, ecology and emerging applications. *Biotechnol. Adv.* 34, 14–29. doi: 10.1016/j.biotechadv.2015.12.003
- Rawlings, N. D., Barrett, A. J., Thomas, P. D., Huang, X., Bateman, A., and Finn, R. D. (2018). The MEROPS database of proteolytic enzymes, their substrates and inhibitors in 2017 and a comparison with peptidases in the PANTHER database. *Nucleic Acids Res.* 46, D624–D632. doi: 10.1093/nar/gkx1134
- Reisky, L., Prechoux, A., Zuhlke, M. K., Baumgen, M., Robb, C. S., Gerlach, N., et al. (2019). A marine bacterial enzymatic cascade degrades the algal polysaccharide ulvan. *Nat. Chem. Biol.* 15, 803–812. doi: 10.1038/s41589-019-0311-9
- Romero, S., Schell, R. F., and Pennell, D. R. (1988). Rapid method for the differentiation of gram-positive and gram-negative bacteria on membrane filters. *J. Clin. Microbiol.* 26, 1378–1382. doi: 10.1128/jcm.26.7.1378-1382.1988
- Rzhetsky, A., and Nei, M. (1992). Statistical properties of the ordinary least-squares, generalized least-squares, and minimum-evolution methods of phylogenetic inference. *J. Mol. Evol.* 35, 367–375. doi: 10.1007/bf00161174
- Saitou, N., and Nei, M. (1987). The neighbor-joining method: a new method for reconstructing phylogenetic trees. *Mol. Biol. Evol.* 4, 406–425. doi: 10.1093/oxfordjournals.molbev.a040454
- Schuerch, M., Spencer, T., and Evans, B. (2019). Coupling between tidal mudflats and salt marshes affects marsh morphology. *Mar. Geology* 412, 95–106. doi: 10.1016/j.margeo.2019.03.008
- Senoura, T., Ito, S., Taguchi, H., Higa, M., Hamada, S., Matsui, H., et al. (2011). New microbial mannan catabolic pathway that involves a novel mannosylglucose phosphorylase. *Biochem. Biophys. Res. Commun.* 408, 701–706. doi: 10.1016/j.bbrc.2011.04.095
- Solanki, V., Kruger, K., Crawford, C. J., Pardo-Vargas, A., Danglad-Flores, J., Hoang, K. L. M., et al. (2022). Glycoside hydrolase from the GH76 family indicates that marine Sulfatibacter sp. Hel_1_6 consumes alpha-mannan from fungi. *ISME J.* 16, 1818–1830. doi: 10.1038/s41396-022-01223-w
- Stam, M., Lelievre, P., Hoebeker, M., Corre, E., Barbeyron, T., and Michel, G. (2023). SulfAtlas, the sulfatase database: state of the art and new developments. *Nucleic Acids Res.* 51, D647–D653. doi: 10.1093/nar/gkac977
- Sun, C., Fu, G. Y., Zhang, C. Y., Hu, J., Xu, L., Wang, R. J., et al. (2016). Isolation and Complete Genome Sequence of *Algibacter alginolytica* sp. nov., a Novel Seaweed-Degrading *Bacteroidetes* Bacterium with Diverse Putative Polysaccharide Utilization Loci. *Appl. Environ. Microbiol.* 82, 2975–2987. doi: 10.1128/AEM.00204-16
- Sun, H., Gao, L., Xue, C., and Mao, X. (2020). Marine-polysaccharide degrading enzymes: Status and prospects. *Compr. Rev. Food Sci. Food Saf.* 19, 2767–2796. doi: 10.1111/1541-4337.12630
- Sun, C., Huo, Y. Y., Liu, J. J., Pan, J., Qi, Y. Z., Zhang, X. Q., et al. (2014). *Thalassomonas eurytherma* sp. nov., a marine proteobacterium. *Int. J. Syst. Evol. Microbiol.* 64, 2079–2083. doi: 10.1099/ijse.0.058255-0
- Sun, C., Xamxidini, M., Wu, Y. H., Cheng, H., Wang, C. S., and Xu, X. W. (2019). *Alteromonas alba* sp. nov., a marine bacterium isolated from seawater of the West Pacific Ocean. *Int. J. Syst. Evol. Microbiol.* 69, 278–284. doi: 10.1099/ijsem.0.003151
- Sun, C., Xu, L., Yu, X. Y., Zhao, Z., Wu, Y. H., Oren, A., et al. (2018). *Minwuiia thermotolerans* gen. nov., sp. nov., a marine bacterium forming a deep branch in the *Alphaproteobacteria*, and proposal of *Minwuiiaceae* fam. nov. and *Minwuiiales* ord. nov. *Int. J. Syst. Evol. Microbiol.* 68, 3856–3862. doi: 10.1099/ijsem.0.003073
- Tabarsa, M., Karnjanapratum, S., Cho, M., Kim, J. K., and You, S. (2013). Molecular characteristics and biological activities of anionic macromolecules from *Codium fragile*. *Int. J. Biol. Macromol.* 59, 1–12. doi: 10.1016/j.jbiomac.2013.04.022
- Tamura, K., Hemswoth, G. R., Dejean, G., Rogers, T. E., Pudlo, N. A., Urs, K., et al. (2017). Molecular mechanism by which prominent human gut bacteroidetes utilize mixed-linkage beta-glucans, major health-promoting cereal polysaccharides. *Cell Rep.* 21, 417–430. doi: 10.1016/j.celrep.2017.09.049

- Tamura, K., Stecher, G., and Kumar, S. (2021). MEGA11: molecular evolutionary genetics analysis version 11. *Mol. Biol. Evol.* 38, 3022–3027. doi: 10.1093/molbev/msab120
- Teeling, H., Fuchs, B. M., Becher, D., Klockow, C., Gardebrecht, A., Bennke, C. M., et al. (2012). Substrate-controlled succession of marine bacterioplankton populations induced by a phytoplankton bloom. *Science* 336, 608–611. doi: 10.1126/science.1218344
- Teeling, H., Fuchs, B. M., Bennke, C. M., Krüger, K., Chafee, M., Kappelmann, L., et al. (2016). Recurring patterns in bacterioplankton dynamics during coastal spring algae blooms. *Elife* 5, e11888. doi: 10.7554/eLife.11888
- Terrapon, N., Lombard, V., Drula, E., Lapebie, P., Al-Masaudi, S., Gilbert, H. J., et al. (2018). PULDB: the expanded database of Polysaccharide Utilization Loci. *Nucleic Acids Res.* 46, D677–D683. doi: 10.1093/nar/gkx1022
- Thongphrom, C., Kim, J. H., and Kim, W. (2016). *Maribacter arenosus* sp. nov., isolated from marine sediment. *Int. J. Syst. Evol. Microbiol.* 66, 4826–4831. doi: 10.1099/ijsem.0.001436
- Unfried, F., Becker, S., Robb, C. S., Hehemann, J. H., Markert, S., Heiden, S. E., et al. (2018). Adaptive mechanisms that provide competitive advantages to marine bacteroidetes during microalgal blooms. *ISME J.* 12, 2894–2906. doi: 10.1038/s41396-018-0243-5
- Weerawongwiwat, V., Kang, H., Jung, M. Y., and Kim, W. (2013). *Maribacter chungangensis* sp. nov., isolated from a green seaweed, and emended descriptions of the genus *Maribacter* and *Maribacter arcticus*. *Int. J. Syst. Evol. Microbiol.* 63, 2553–2558. doi: 10.1099/ijms.0.039628-0
- Wolter, L. A., Mitulla, M., Kalem, J., Daniel, R., Simon, M., and Wietz, M. (2021). CAZymes in *maribacter dokdonensis* 62-1 from the patagonian shelf: genomics and physiology compared to related flavobacteria and a co-occurring *alteromonas* strain. *Front. Microbiol.* 12, 628055. doi: 10.3389/fmicb.2021.628055
- Wu, Z. C., Zhang, X. Y., Sun, C., Xu, L., Fu, G. Y., and Xu, X. W. (2021). *Aestuarius baculum sediminum* sp. nov., a marine bacterium isolated from a tidal flat in Zhoushan. *Arch. Microbiol.* 203, 2953–2960. doi: 10.1007/s00203-021-02262-1
- Xie, J., Chen, Y., Cai, G., Cai, R., Hu, Z., and Wang, H. (2023). Tree Visualization By One Table (tvBOT): a web application for visualizing, modifying and annotating phylogenetic trees. *Nucleic Acids Res.* 51, W587–W592. doi: 10.1093/nar/gkad359
- Xing, P., Hahnke, R. L., Unfried, F., Markert, S., Huang, S., Barbeyron, T., et al. (2015). Niches of two polysaccharide-degrading *Polaribacter* isolates from the North Sea during a spring diatom bloom. *ISME J.* 9, 1410–1422. doi: 10.1038/ismej.2014.225
- Xu, L., Ying, J. J., Fang, Y. C., Zhang, R., Hua, J., Wu, M., et al. (2021). *Halomonas populi* sp. nov. isolated from *Populus euphratica*. *Arch. Microbiol.* 204, 86. doi: 10.1007/s00203-021-02704-w
- Xu, T., Yu, M., Lin, H., Zhang, Z., Liu, J., and Zhang, X. H. (2015). Genomic insight into *Aquimarina longa* SW024 T: its ultra-oligotrophic adapting mechanisms and biogeochemical functions. *BMC Genomics* 16, 772. doi: 10.1186/s12864-015-2005-3
- Xue, C. X., Zhang, H., Lin, H. Y., Sun, Y., Luo, D., Huang, Y., et al. (2020). Ancestral niche separation and evolutionary rate differentiation between sister marine flavobacteria lineages. *Environ. Microbiol.* 22, 3234–3247. doi: 10.1111/1462-2920.15065
- Ying, J. J., Fang, Y. C., Ye, Y. L., Wu, Z. C., Xu, L., Han, B. N., et al. (2021). *Marinomonas vulgaris* sp. nov., a marine bacterium isolated from seawater in a coastal intertidal zone of Zhoushan island. *Arch. Microbiol.* 203, 5133–5139. doi: 10.1007/s00203-021-02500-6
- Yoon, J. H., Kang, S. J., Lee, S. Y., Lee, C. H., and Oh, T. K. (2005). *Maribacter dokdonensis* sp. nov., isolated from sea water off a Korean island, Dokdo. *Int. J. Syst. Evol. Microbiol.* 55, 2051–2055. doi: 10.1099/ijms.0.63777-0
- Zeugner, L. E., Krüger, K., Barrero-Canosa, J., Amann, R. I., and Fuchs, B. M. (2021). *In situ* visualization of glycoside hydrolase family 92 genes in marine flavobacteria. *ISME Commun.* 1, 81. doi: 10.1038/s43705-021-00082-4
- Zhang, X., Hu, B. X., Ren, H., and Zhang, J. (2018b). Composition and functional diversity of microbial community across a mangrove-inhabited mudflat as revealed by 16S rDNA gene sequences. *Sci. Total Environ.* 633, 518–528. doi: 10.1016/j.scitotenv.2018.03.158
- Zhang, G. I., Hwang, C. Y., Kang, S. H., and Cho, B. C. (2009). *Maribacter antarcticus* sp. nov., a psychrophilic bacterium isolated from a culture of the Antarctic green alga *Pyramimonas gelidicola*. *Int. J. Syst. Evol. Microbiol.* 59, 1455–1459. doi: 10.1099/ijms.0.006056-0
- Zhang, J. Y., Xia, Y., Feng, X., Mu, D. S., and Du, Z. J. (2020). *Maribacter algarum* sp. nov., a new member of the family *Flavobacteriaceae* isolated from the red alga *Gelidium amansii*. *Int. J. Syst. Evol. Microbiol.* 70, 3679–3685. doi: 10.1099/ijsem.0.004220
- Zhang, H., Yohe, T., Huang, L., Entwistle, S., Wu, P., Yang, Z., et al. (2018a). dbCAN2: a meta server for automated carbohydrate-active enzyme annotation. *Nucleic Acids Res.* 46, W95–W101. doi: 10.1093/nar/gky418
- Zhu, Y., Suits, M. D., Thompson, A. J., Chavan, S., Dinev, Z., Dumon, C., et al. (2010). Mechanistic insights into a Ca²⁺-dependent family of alpha-mannosidases in a human gut symbiont. *Nat. Chem. Biol.* 6, 125–132. doi: 10.1038/nchembio.278
- Zhu, Y., Thomas, F., Larocque, R., Li, N., Duffieux, D., Cladiere, L., et al. (2017). Genetic analyses unravel the crucial role of a horizontally acquired alginate lyase for brown algal biomass degradation by *Zobellia galactanivorans*. *Environ. Microbiol.* 19, 2164–2181. doi: 10.1111/1462-2920.13699